available at www.sciencedirect.com

ScienceDirect

www.elsevier.com/locate/brainres

BRAIN RESEARCH

Research Report

Individual differences in risk preference predict neural responses during financial decision-making

Jan B. Engelmann[a,*], *Diana Tamir*[b]

[a]*Department of Psychiatry and Behavioral Sciences, Emory University School of Medicine, 101 Woodruff Circle, Atlanta, GA 30329, USA*
[b]*Department of Psychology, Harvard University, 33 Kirkland Street, Cambridge, MA 02138, USA*

ARTICLE INFO

Article history:
Accepted 23 June 2009
Available online 2 July 2009

Keywords:
Decision-making
fMRI
Risk
Task phase
Expected utility
Individual differences
Anterior cingulate cortex
Posterior cingulate cortex

ABSTRACT

We investigated the neural correlates of subjective valuations during a task involving risky choices about lotteries. Because expected value was held constant across all lotteries, decisions were influenced by subjective preferences, which manifest behaviorally as risk-seeking or risk-averse attitudes. To isolate structures encoding risk preference during choice, we probed for areas showing increased activation as a function of selected risk-level. Such response patterns were obtained in anterior (ACC) and posterior cingulate cortex (PCC), superior frontal gyrus, caudate nucleus, and substantia nigra. Behavioral results revealed the presence of risk-averse and risk-neutral individuals. In parallel, brain signals revealed modulation of activity by risk attitude during choice. Correlations between risk-seeking attitudes and neural activity during risky choice were obtained in superior and inferior frontal gyri, medial and lateral orbitofrontal cortex, and parahippocampal gyrus, while correlations with risk-averse attitudes were found in the caudate. The dynamics of neural responses relevant to each stage of the task (decision, anticipation, outcome) were investigated via timeseries and conjunction analyses. Though the networks engaged in each of the task stages were mostly distinct, regions within ACC, PCC and caudate were consistently activated during each decision-making phase. These results demonstrate (1) that subjective assessments of risk, as well as individual attitudes toward risk, play a significant role in modulating activity within brain regions recruited during decision-making, and (2) that ACC, PCC and caudate are relevant during each phase of a decision-making task requiring subjective valuations, strengthening the role of these regions in self-referential subjective valuations during choice.

1. Introduction

The majority of our everyday decisions involve some level of risk. Decision-making under risk is a complex process and both cognitive and emotional factors are involved in the selection of goal-directed responses (Kahneman and Tversky, 1979; Loewenstein et al., 2001; Mellers, 2000). In order to maximize rewards, a decision maker needs to evaluate alternative courses of actions whose outcomes are uncertain. According to classical expected utility theory, the standard microeconomic model of choice under risk, such valuations involve estimations of the reward magnitude and likelihood with which some outcome can be obtained. The multiplicative product of objective reward magnitude and likelihood is referred to as *expected value* (Bernoulli, 1958; von Neumann and Morgenstern, 1944). Expected Utility Theory (EUT) has

* *Corresponding author*. Fax: +1 404 727 3233.
E-mail address: jan.engelmann@emory.edu (J.B. Engelmann).

0006-8993/$ – see front matter © 2009 Elsevier B.V. All rights reserved.
doi:10.1016/j.brainres.2009.06.078

proven to be a useful construct for predicting animal and human choices (Camerer, 2003). Importantly, the utility of obtaining a given outcome can be influenced by subjective factors determining the "moral", or subjective, value of a lottery (Kable and Glimcher, 2007; Schunk and Betsch, 2006; Trepel et al., 2005). An influential factor is a person's preference for risk. Results from previous research indicate that most people show risk-averse attitudes when gambling for monetary gains, which is reflected by a concave utility function (Abdellaoui, 2000; Gonzales and Wu, 1999; Tversky and Fox, 1994). Various experiments, however, have reported heterogeneity in risk attitudes across individuals (e.g. Fetherstonhaugh et al., 1997; Huettel et al., 2006; Schunk and Betsch, 2006). Results from these experiments support the notion that individuals not only estimate expected value, but more importantly, they seem to weigh these estimates by *subjective* factors, such as risk preference (Kahneman and Tverksy, 1979; Schunk and Betsch, 2006) and the anticipated pleasure (Mellers, 2001) and dread (Berns et al., 2006) of the outcome. Due to the subjective nature of these variables, these estimates can vary from person to person and thus influence individual's decisions to different degrees. Such heterogeneity in risk attitudes across individuals has been demonstrated in behavioral economics and neuroeconomics (e.g. Barsky et al., 1997; Beetsma and Schotman, 2001; Huettel et al., 2006; Kachelmeier and Shehata, 1992; Schunk and Betsch, 2006).

In the current experiment, we set out to investigate the neural correlates of individual differences in risk attitude employing a two-choice financial decision-making task between lotteries involving risk. This task is well-established in behavioral economics and allows for the extraction of factors that can influence choice, particularly risk preference. Here, we created a setting within which participants were asked to make binary choices between lottery pairs of *equal* expected value. Lotteries varied in reward magnitude and winning probability, such that one of the lotteries yielded a higher payoff at a comparatively large risk, while the other yielded a lower payoff, but involving less risk. Because in the context of the current paradigm decisions were not influenced by the expected value of lotteries, which was equal for all decisions, but by subjective factors involved in participant's valuations of lottery pairs, e.g. risk attitude, we created a setting ideal for investigating the neurobiological basis of individual differences in risk preference. We extracted risk preference from participants' choices during scanning using nonlinear logistic regression. This approach provided individualized risk preference parameters, which characterize the curvature of participants' utility functions. We then examined the neural basis of risk preference by regressing each participant's behavioral risk preference parameter against neural activations during risky choice. Finally, we investigated activation patterns in these regions separately for risk-averse and risk-seeking individuals to illustrate differential activation patterns as a function of risk attitude.

In the second part of this paper, we made use of the event-related fMRI design employed in the current experiment to investigate potential differences and similarities in networks recruited during component phases of decision-making under risk (Fig. 1). Component phases include (1) a selection phase during which choices between the two lotteries were made, (2) reward anticipation and (3) the outcome phase, during which the outcome of the chosen gamble was presented resulting in either receipt or omission of the anticipated cash reward (e.g. Ernst et al., 2004; Knutson et al., 2000, 2001a). While previous research has dissociated different phases of decision-making under uncertainty (e.g. Liu et al., 2007; for review see also Knutson and Cooper (2005)), to our knowledge, this is the first study on decision-making under risk investigating the dynamics of all three task phases.

The selection phase requires the evaluation of sensory input based on prior knowledge and experiences made in similar situations (Platt, 2002). A course of action is then chosen from potential alternatives. During this evaluatory period, an anticipation of the potential outcome is formed on the basis of probabilities of expected outcomes and the magnitude of the reward in conjunction with previous experiences (Ernst et al., 2004; Mellers, 2001; Platt and Glimcher, 1999). Based on previous research on risky decision-making (e.g. Cohen and Ranganath, 2005; Huettel et al., 2005; Paulus and Frank, 2006; Preuschoff et al., 2006), we expected the choice evaluation network to include anterior insula, the anterior cingulate cortex, ventral and dorsal striatum, and posterior cingulate and orbitofrontal cortex. During the second phase, reward anticipation is maintained until the outcome period and typically involves activation of ventral striatum, whose importance in computing reward expectancy has been demonstrated by both monkey electrophysiology (Mirenowicz and Schultz, 1996; Schultz et al., 1992, 1997) and human neuroimaging studies (e.g. Knutson et al., 2001a, 2005). We also expected to observe activations in areas involved in sustained attention, such as parietal cortex (Corbetta et al., 2000; Engelmann et al., 2009; Hopfinger et al., 2000; Pessoa et al., 2002). Finally, during the outcome period, risk is resolved and an evaluation of the obtained result takes place. This involves a comparison between the expected outcome and the actual outcome. The discrepancy between expected and obtained outcomes forms the prediction error, which is a key term in computational models of reinforcement learning (Montague and Berns, 2002; Montague et al., 2004; Schultz and Dickinson, 2000). The reward prediction error provides the basis for adjustments of future behavior and reward expectation (e.g. Hollerman et al., 1998; McClure et al., 2003; O'Doherty et al., 2003b; Seymour et al., 2004) and has been shown to engage ventral striatum (McClure et al., 2003; Menon et al., 2007; O'Doherty et al., 2003b) and orbitofrontal cortex (O'Doherty et al., 2003b).

To extract the network encoding risk preference during choice, we sorted trials based on the decisions made by subjects and then probed for brain regions showing linear increases in activation as a function of relative risk-level selected by participants during decision and anticipation phases. We hypothesized that risky choices between lotteries of equal expected value would lead to differential brain activations in regions encoding *subjective* valuations concerning a trade-off between risk-level and gain magnitude of the chosen lottery. In order to examine the relative involvement of each area during different phases of our task, we investigated activation patterns within each of the task phases using deconvolved time courses spanning the entire trial length. This allowed us to examine whether regions activated during

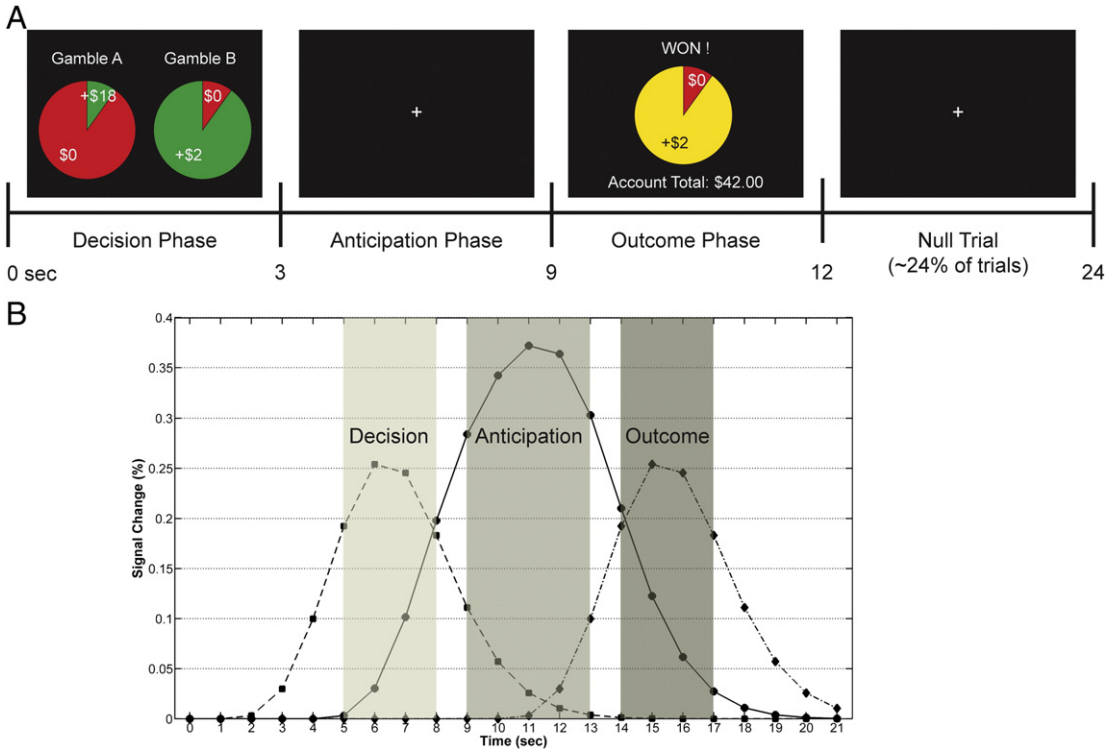

Fig. 1 – Experimental design. (A) Schematic outline and timing of task phases. Each trial began with the presentation of a gamble pair during which participants chose their preferred gamble, followed by an anticipation period. At the end of each trial, participants were shown the outcome of the selected trial, together with their cumulative earnings (account total). In addition, null trials followed about 24% of task trials. (B) Time course representing expected activation for each task phase. The grey areas represent the time periods during which peaks of activation for each phase are expected, based on a canonical HRF model using a gamma variate function. Hemodynamic responses are expected to peak starting about 5 s after image onset during decision and outcome phases; the response peak during the anticipation period is centered between these two task phases.

one phase also showed increased activations during other phases. Results from time course analyses were corroborated by conjunction analyses, which allowed us to inspect the relative spatial overlap between activation clusters observed in different task phases.

2. Results

2.1. *Behavior*

Risk-sensitivity was assessed by fitting nonlinear logistic regression to each participant's choices collected during scanning. We computed the curvature of the utility function, as outlined in detail above, which yielded a median α of 1.0766 (mean=0.8796, range: 0.2603 to 1.2808). This finding indicates that most participants in the current study were risk-neutral to mildly risk-seeking, while a subsample was risk-averse (Fig. 2, Table 1). Importantly, our results demonstrate a range of risk attitudes that include risk-aversion, risk-neutrality and mildly risk-seeking attitudes and are apparent in both α values estimated by nonlinear logistic regression and proportion of risky choices. These results are in agreement with previous research (e.g. Fetherstonhaugh et al., 1997; Schunk and Betsch, 2006) and underline the importance of subjective factors in economic choice in the context of the current experiment. Finally, no significant reaction time differences were obtained [Mean RTs: 1147 ms (CO), 1180 ms (LR), 1179 ms (HR)]. Taken together, our behavioral data demonstrate heterogeneity in risk attitude in accordance with previous findings (e.g. Schunk and Betsch, 2006; Tversky and Kahnemann, 1981).

2.2. *fMRI*

2.2.1. *Neural correlates of risk preference during choice*

In this part, we report results on the neural correlates of relative behavior risk during the decision period. First, we outlined a network of structures that showed significant activation increases as a function of the selected risk-level during choice. We then considered a separate network in which activity is modulated by individual differences in risk preference. Finally, we investigated activation patterns in this network separately for risk-averse and risk-seeking individuals in order to illustrate differential activation patterns as a function of risk attitude.

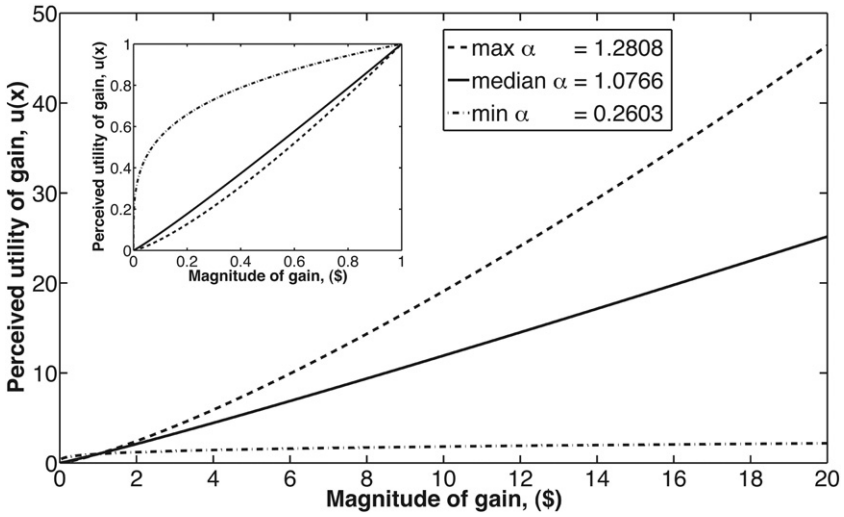

Fig. 2 – Behavior. When modeled as a power function, the curvature of the utility function is determined by the value of its exponent (α), which represents how relatively risk-seeking ($\alpha>1$), risk-neutral ($\alpha=1$), or risk-averse ($\alpha<1$) an individual's behavior is. The curvature of the utility function was extracted from behavioral responses of each subject using nonlinear logistic regression. Overall, the group was risk-neutral to mildly risk-seeking (median $\alpha=1.0766$, solid line), but subjects showed heterogeneous risk-related behavior, ranging from relatively risk-averse (min $\alpha=0.2603$, dotted line) to risk-seeking (max $\alpha=1.2808$, dashed line). The graph inset shows the curvature of the utility functions for values below 1.

2.2.1.1. Decision phase activations as a function of risky choice. As predicted by our hypothesis, areas that encoded relative behavioral risk during the decision phase of the current task were obtained in a network of structures typically associated with conflict monitoring, such as the anterior cingulate cortex, task control and selection of action sets, such as the superior frontal gyrus (including activation centers in BA6, BA8, and BA9) and right posterior cingulate cortex, and reward processing, such as the caudate nucleus and an area in the brainstem that is consistent with the substantia nigra (Fig. 3A). Increased activations were also obtained in the thalamus, as well as regions associated with visual and attentional processing including precuneus, middle occipital gyrus, parahippocampal gyrus and fusiform gyrus (Table 2). To illustrate activation patterns within regions encoding relative behavioral risk during choice, time series were extracted for each subject as a function of CHOICE (control, low-risk and high-risk choice) and are shown in Fig. 3B. Patterns reflected in deconvolved time courses show increased activations around the expected peak during the decision phase as a function of risk-level, with a large peak during risky decisions, a smaller peak during low-risk decisions, and a further decrease in peak BOLD responses during control choices. This activation pattern indicates that these regions are involved in risky decision-making. This is further supported by trend analyses of mean peak activations indicating significant linear increases as a function of relative behavioral risk in the network of structures shown in Fig. 3C: posterior cingulate cortex [$F(1,8)=111.18$, $p<0.001$, $\eta^2=0.933$], anterior cingulate cortex [$F(1,8)=79.238$, $p<0.001$, $\eta^2=0.908$], caudate nucleus [$F(1,8)=18.672$, $p<0.005$, $\eta^2=0.70$], substantia nigra [$F(1,8)=34.92$, $p<0.001$, $\eta^2=0.814$], and superior frontal gyrus [BA6: $F(1,8)=28.046$, $p<0.001$, $\eta^2=0.778$; BA8: $F(1,8)=26.108$, $p<0.001$, $\eta^2=0.765$; BA9: $F(1,8)=26.110$, $p<0.001$, $\eta^2=0.765$]. These findings were supported by ROI analyses of the parametric effects of risk, which indicate that mean regression coefficients were significantly greater than zero in all regions (Table 2).

We also investigated the effect of scanning environment on these activation patterns in regions of interest. Except for two areas (PCC, SFG/BA9), no significant effects of the factor SESSION were obtained. In the PCC, a near-significant main effect of SESSION was observed [$F(1,8)=8.696$, $p=0.016$, $\eta^2=0.521$], with greater mean activation in the BrU sample (0.167) compared to the IU sample (0.094). No significant interactions with the factor SESSION were observed, indicating that this factor did not affect activation trends within the PCC. In the SFG/BA9, we did obtain a near-significant interaction between CHOICE and SESSION [$F(1,8)=9.255$, $p=0.016$, $\eta^2=0.536$], indicating different trends of activation within different scanning environments. We therefore performed separate trend analyses on our two samples and found a significant

Table 1 – Alpha values estimated by nonlinear logistic regression and proportion risky choices across all subjects.

Subject	Alpha	Proportion risky choice
IU1	0.2603	0.1417
IU2	1.0932	0.5417
IU3	1.1361	0.5583
IU4	1.2292	0.5917
IU5	1.2808	0.5254
IU6	1.0599	0.5759
BrU1	0.2719	0.1100
BrU2	1.1294	0.5500
BrU3	0.9725	0.4433
BrU4	0.3624	0.3000

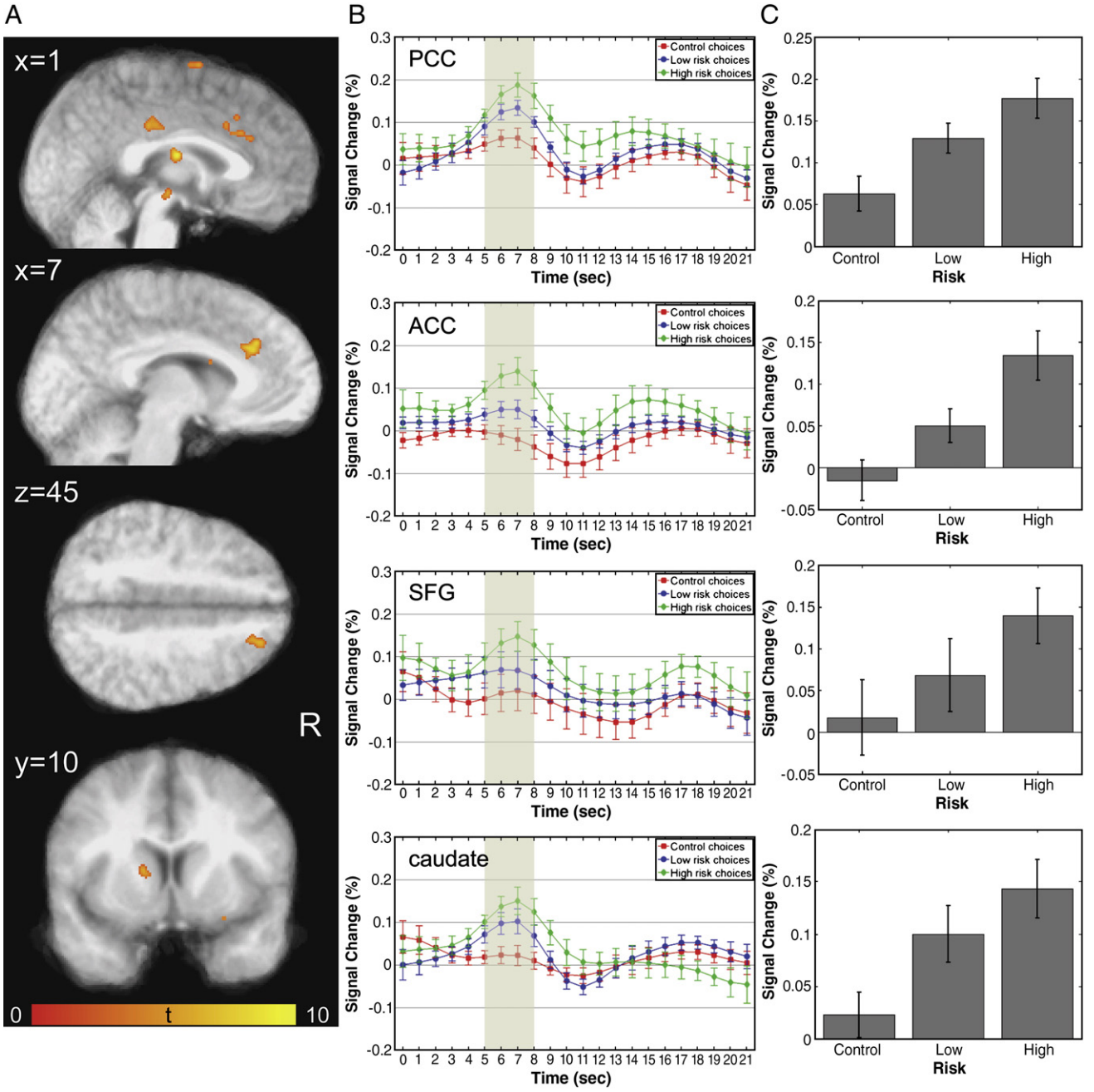

Fig. 3 – Neural correlates of risky choice during the decision phase. (A) Plots show regions with activations during the decision phase of the task that were significantly modulated by relative behavioral risk associated with a subject's choice (high-risk, low-risk, or control). Areas demonstrating this risk-related encoding include posterior cingulate (PCC), anterior cingulate (ACC), superior frontal gyrus (SFG), caudate, substantia nigra, and thalamus. For a complete list of regions showing risk-related modulation during decision-making, see Table 2. The color bar represents *t* values. (B) Timeseries of activations for each type of decision, high-risk (green), low-risk (blue), and control (red), for four regions, PCC, ACC, SFG (averaged across two adjacent activation clusters in BA8 and BA9) and the caudate nucleus. All regions illustrate significant risk-related modulation of neural activation intensity, with high-risk-choices eliciting the greatest response. (C) Mean peak activations in each of the regions represented in (B). In all regions, neural responses follow a significant linear trend of increasing activation with increasing relative behavioral risk.

linear trend for the IU sample [$F(1,5)=31.578$, $p<0.005$, $\eta^2=0.863$], while the BrU sample did not show a significant linear trend [$F(1,3)=3.754$, $p=0.148$, $\eta^2=0.556$]. Mean activations within each condition show that, even in the BrU sample, this area still distinguished between high-risk decisions versus low-risk and control decisions (CO: 0.141, LR: 0.131, HR: 0.182). This is most likely due to the presence of an equal amount of risk-seeking and risk-averse individuals in

Table 2 – Areas showing significant activations during risky choice.

Structure	L/R	BA	Volume	X	Y	Z	Max T	Parametric effects	
								$Mean_{slope}$	T_{slope}
Superior frontal gyrus	R	9	108	24.8	48	32.6	6.0859	0.013	2.862*
Superior frontal gyrus	R	8	270	19.8	33.9	45.4	5.9561	0.017	6.477****
Anterior cingulate cortex	R	32	81	11.6	33.5	−0.5	6.1647	0.020	3.914***
Middle frontal gyrus	R	11	81	29.7	32.4	−12.5	9.9459	0.006	2.369*
Anterior cingulate cortex	R	32	108	12	28.5	30.9	6.5979	0.031	2.606*
Anterior cingulate cortex	Bi	32	1242	−4.1	26.8	28.5	9.4219	0.031	4.546****
Caudate nucleus	L		108	−12.8	9.8	10	6.0093	0.035	3.506**
Posterior orbital gyrus	R		81	25.5	7.5	−12.5	5.2881	0.005	2.209n.s.
Caudate nucleus	L		81	−7.8	7.5	21.4	7.5513	0.031	2.628*
Superior frontal gyrus	R	6	108	9.7	5.2	65.5	5.9678	0.022	3.352**
Supplementary motor area (SFG)	R	6	108	0.6	−0.6	68.5	7.5092	0.028	3.559**
Thalamus	Bi		297	0.9	−12.5	17.5	10.081	0.036	3.635***
Brainstem (substantia nigra)	R		135	1.5	−17.1	−4.7	6.1395	0.036	3.445**
Posterior cingulate cortex	R	23	243	1.8	−25	34.2	6.0447	0.022	4.538****
Parahippocampal gyrus	L	30	270	−17.1	−35.1	4.3	6.6059	0.026	3.630***
Parahippocampal gyrus	R	30	135	18.9	−36.3	5.5	5.9321	0.020	5.034****
Cerebelum	R		81	18.6	−47.6	−20.6	6.0407	0.010	2.608*
Fusiform gyrus	R	37	216	24.4	−47.7	−14	6.6265	0.020	4.633****
Fusiform gyrus	L	37	405	−38.2	−57.1	−3	6.852	0.015	5.763****
Precuneus	L	7	81	−17.4	−65.6	39.4	6.0629	0.001	4.570****
Inferior occipital gyrus	R	19	702	42	−70.2	−2.5	8.0636	0.018	4.776****
Cuneus	L	18	81	−16.5	−71.5	18.5	5.5186	0.013	6.498****
Precuneus	L	19	81	−26.4	−75.4	35.5	6.2081	0.033	2.652*
Middle occipital gyrus	R	19	243	32.8	−82.9	12.5	6.5496	0.032	3.967***
Middle occipital gyrus	L	19	756	−31.7	−83.6	11.8	7.2461	0.020	7.739****

Volume (in μl), Talairarch coordinates of activation peaks, and results from ROI analyses of the parametric effects of risk (mean slope as well as significance level) are also shown.
n.s.: near-significant; *: significant at $p<0.05$; **: significant at $p<0.01$; ***: significant at $p<0.005$; ****: significant at $p<0.001$.

the BrU sample (see Table 1, Fig. 5). These 2 groups show opposite activation patterns (Fig. 5) that may average out the linear trend in the BrU sample. Taken together, these findings indicate that differences in scanning environments had a negligible effect on activation trends during the decision phase of the current study.

2.2.1.2. Neural correlates of risk preference. Next, we investigated the extent to which individual differences in activations during risky decision-making were related to individual differences in behavioral risk preference by correlating participants' risk-aversion parameters estimated using nonlinear logistic regression with BOLD responses due to relative behavioral risk. As shown in Fig. 4, areas whose neural responses during risky choice were significantly modulated by risk preference included medial orbitofrontal cortex, right superior frontal gyrus, left inferior frontal gyrus, bilateral BA47, caudate and bilateral parahippocampal gyrus (see also Table 3). Scatterplots shown in Fig. 4 illustrate activation patterns within this network, showing average regression coefficients (beta weights) for the contrast comparing high-risk to control choice plotted as a function of participants' risk preference together with the line of best fit. Partial correlation analyses, controlling for the effect of session, indicated significant positive modulations of neural responses during risky choice by behavioral risk preference in the following network of structures: medial orbitofrontal cortex ($r=0.9902$, $p<0.001$), right superior frontal gyrus ($r=0.9413$, $p<0.001$), left inferior frontal gyrus ($r=0.9359$, $p<0.001$), bilateral BA47 (left: $r=0.961$, $p<0.001$; right: $r=0.889$, $p<0.001$) and bilateral parahippocampal gyrus (left: $r=0.9421$, $p<0.001$; right: $r=0.9322$, $p<0.001$). Significant negative modulations of neural responses during risky choice by behavioral risk preference were obtained in the right caudate nucleus ($r=-0.9392$, $p<0.001$). Of note, a region in right anterior insula (peak voxel at 34,10,14; Max t: 5.59) also showed negative modulations of BOLD responses during risky decisions by risk preference, but did not survive the selected cluster-size threshold at the selected α-value. These findings indicate that activations during risky choice were modulated by subjectwise parameters reflecting individual differences in risk preference. These findings were corroborated by confirmatory bootstrap analyses on Pearson's rho (see Table 3). Specifically, bootstrap analyses were conducted on Pearson's rho in all regions of interest without replacement ($N=10$, 10,000 repetitions). Except for two regions, namely orbitofrontal gyrus and thalamus, correlation coefficients in all of these areas surpassed the alpha level of 0.05, as indicated by mean rho values falling within the 95% confidence intervals, which were estimated using the corrected and accelerated percentile method (Table 3).

2.2.1.3. ROI analyses of areas showing activation differences as a function of behavioral risk preference. The scatterplots shown in Fig. 4 and the behavioral data shown in Table 1 indicate a clustering of the data into participants that are risk-neutral to mildly risk-seeking (risk seekers) and participants that are risk-averse (risk averters). To confirm such clustering,

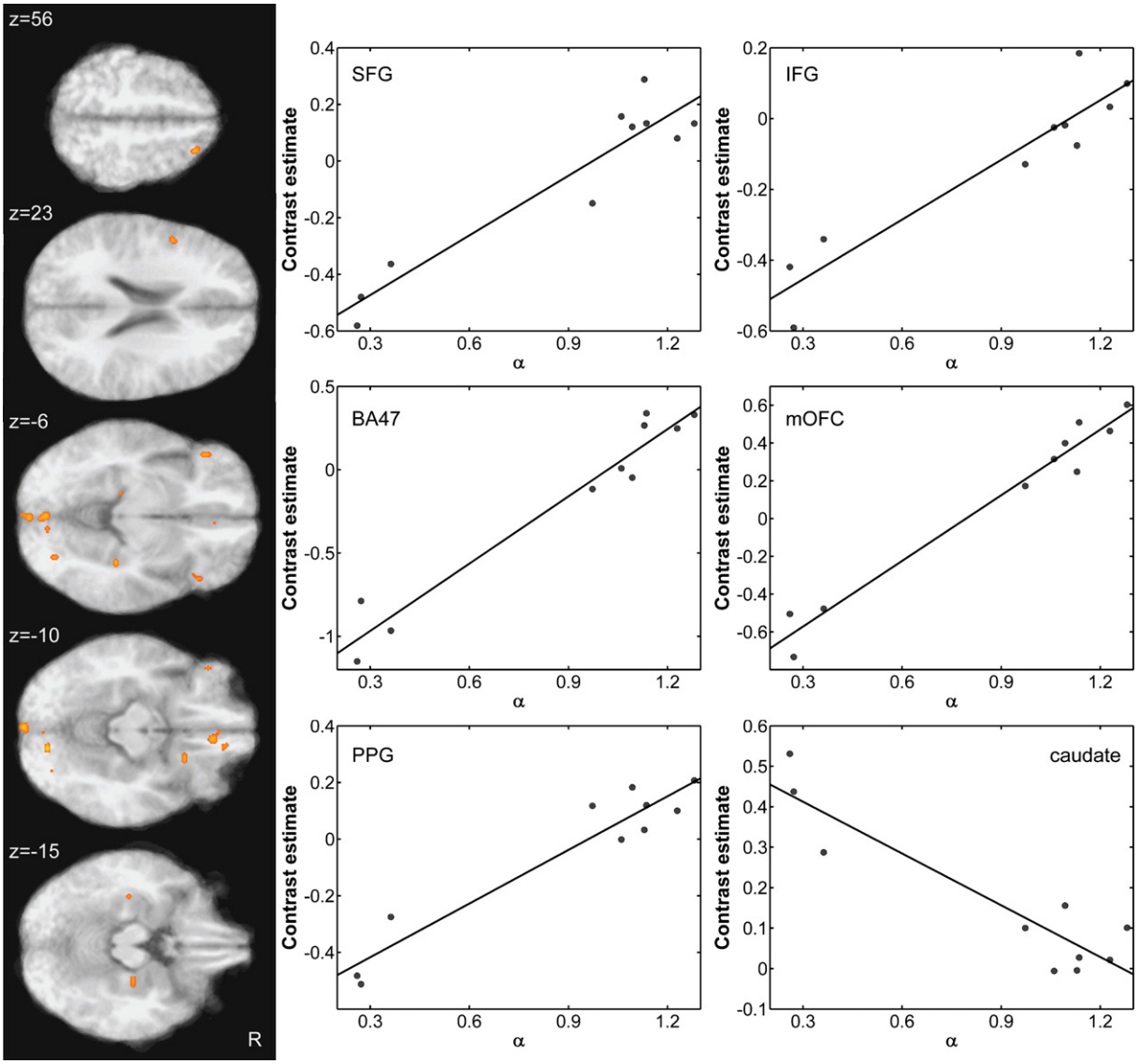

Fig. 4 – Neural correlates of risk preference. Behaviorally derived measures of individual risk preference significantly modulated the neural responses during risky choices in a network of structures that included superior frontal gyrus (SFG), inferior frontal gyrus (IFG), bilateral orbitofrontal cortex/BA47, medial orbitofrontal cortex (mOFC), parahippocampal gyrus (PPG), and the caudate nucleus. Scatterplots on the right show individual subject's contrast estimates (betas) regressed against behavioral risk preference, *α*. Significant correlations between behavioral risk preference and neural activity were found in each of the illustrated areas. All correlations were positive, indicating increased BOLD activations with increased risk-seeking behavior, except for the caudate, which showed the opposite relationship.

we conducted cluster analysis on each individual's mean activation of the entire risk preference network outlined in the previous section and risk-aversion parameter (α). Cluster analysis confirmed the division of the data set into two categories: risk seekers ($n=7$) vs. risk averters ($n=3$, Fig. 5A). An independent samples t-test, indicating a significantly greater mean α for risk seekers (1.129) compared to risk averters (0.298), further verified this clustering [$t(8)=12.87$, $p<0.001$).

To investigate the extent to which brain responses in these areas distinguished between risk averters and risk seekers, we conducted ROI analyses. First, mean responses during control, low-risk and high-risk choices were extracted for each group. We then probed for differences in activation trends across risk seekers and risk averters in the network of structures showing a *positive* correlation with behavioral risk preference. The caudate nucleus, which showed a *negative* correlation with behavioral risk preference, was analyzed separately. In particular, we probed these regions for a significant interaction between CHOICE and GROUP using linear trend analysis. Such interaction is indicative of activation pattern differences as a function of GROUP. When considering activity in the whole network (Fig. 5B), linear trend analysis yielded a significant interaction between CHOICE and GROUP, indicating significant differences in linear trends as a function of risky choice in risk averters and risk seekers [$F(1,8)=198.61$, $p<0.001$, $\eta^2=0.96$]. To further investigate the nature of this interaction, a one-way

Table 3 – Areas showing significant correlations between risk preference and activation during risky choice.

Structure	L/R	BA	Volume	X	Y	Z	Max T	ρ_{part}	ρ_{boot}	95% CI_{boot}	
										Lower Lim.	Upper Lim.
Orbitofrontal gyrus	R	32	81	11.5	44.5	−9.5	5.3174	0.8975	0.888	−0.6978	0.98048
Medial orbitofrontal cortex	R	32	270	5.4	37.8	−10.4	7.079	0.9902	0.979*	0.64449	0.99295
Inferior frontal gyrus/lateral orbitofrontal gyrus	L	47	135	−43.5	31.9	−7.5	8.2192	0.961	0.945*	0.5289	0.98387
Inferior frontal gyrus/lateral orbitofrontal gyrus	R	47	81	42.6	25.5	−6.5	6.1803	0.8889	0.899*	0.53128	0.97669
Superior frontal gyrus	R	6	81	21.7	24.3	56.5	8.1419	0.9413	0.924*	0.43255	0.98181
Lentiform nucleus/putamen	R		81	19.6	16.5	−9.5	7.8898	0.9348	0.944*	0.34819	0.97172
Caudate	R		108	14.2	9.7	15.2	−5.6649	−0.9392	−0.893*	−0.97317	−0.06868
Inferior frontal gyrus	L	9	81	−47.5	8.4	23.5	6.4359	0.9359	0.936*	0.27139	0.97541
Parahippocampal gyrus	R	35	81	25.2	−19.5	−15.5	6.7047	0.9322	0.918*	0.00095	0.9801
Parahippocampal gyrus	L	36	81	−33.6	−21.6	−17.3	7.4711	0.9421	0.925*	0.50077	0.98746
Thalamus	L		81	−15.6	−26.6	−4.6	5.9339	0.9084	0.896	−0.19257	0.97983
Hippocampus	R		81	32.4	−31.5	−5.6	7.6215	0.9369	0.944*	0.6549	0.98487
Fusiform gyrus	R	19	81	28.5	−75.3	−7.4	7.3343	0.9369	0.929*	0.23533	0.98649
Lingual gyrus	R	18	108	11.1	−79.5	−8.4	11.617	0.9445	0.942*	0.55701	0.99457
Inferior occipital gyrus	L	18	81	−34.3	−79.5	−3.5	7.2258	0.9253	0.899*	0.23477	0.97682
Lingual gyrus	Bi	18	189	0.5	−82.4	−7.6	7.3588	0.9361	0.937*	0.16037	0.97746
Lingual gyrus	Bi	18	324	−0.9	−94.5	−7.9	7.7466	0.9278	0.941*	0.35487	0.96984

Volume (in μl), Talairach coordinates of the activation peak and results from ROI analyses are also displayed: Pearson's partial correlation coefficient (ρ_{part}) and confirmatory bootstrap analyses on Pearson's rho (ρ_{boot}) with 95% confidence intervals.
* Significant at $p<0.05$ as estimated by confirmatory bootstrap analyses.

between-subjects ANOVA was conducted at each risk-level (control, low-risk, high-risk). Significantly greater mean activation in the network for risk seekers (0.772) compared to risk averters (0.293) was obtained in the high-risk condition [$F(1,8)=5.516$, $p<0.05$, $\eta^2=0.41$]. No significant group differences were obtained during control and low-risk choices. When considering activity in the caudate nucleus, trend analyses revealed a similar interaction, but in the opposite direction [$F(1,8)=6.32$, $p<0.05$, $\eta^2=0.44$] (Fig. 5C). A one-way between-subjects ANOVA revealed significantly greater mean activation when participants selected the high-risk option for risk averters (0.163) compared to risk seekers (0.065) [$F(1,8)=5.477$, $p<0.05$, $\eta^2=0.41$], while no other significant group differences were obtained. Fig. 5B shows mean activity in the whole risk preference network and Fig. 5C shows activity in the caudate nucleus. Of note, compared to network activations, opposite activation patterns were observed in the caudate, with activity increasing as a function of risky choice in risk averters, while this was not the case for risk-seeking individuals.

Finally, we investigated individual ROIs in the risk preference network. Trend analyses indicated that all regions showed a significant interaction between CHOICE and GROUP, however, a subset of regions showed maximally different activation patterns across these two groups. These regions either showed significant group differences during control or high-risk choices, indicative of activity decreasing as a function of risky choice in risk averters, while activity increased as a function of risky choice in risk seekers. Such activation patterns were observed in left BA47, with significantly greater activity for risk averters (0.543) compared to risk seekers (0.10) in the control condition and near-significantly smaller activity during high-risk choices for risk averters (−0.477) compared to risk seekers (0.107) [CO: $F(1,8)=8.041$, $p<0.05$, $\eta^2=0.50$; HR: $F(1,8)=4.897$, $p=0.058$, $\eta^2=0.38$]. In medial orbitofrontal cortex and putamen, significant group differences were obtained during high-risk choices [mOFC: HR: $F(1,8)=6.027$, $p<0.05$, $\eta^2=0.43$; putamen: HR: $F(1,8)=8.096$, $p<0.05$, $\eta^2=0.50$], with risk seekers (mOFC: 0.549, putamen: 0.318) showing significantly greater activity than risk averters (mOFC: −0.344; putamen: −0.578). Finally, superior frontal gyrus showed a significant group effect during high-risk choices [$F(1,8)=5.494$, $p<0.05$, $\eta^2=0.41$], with greater activity obtained for risk seekers (−0.161) compared to risk averters (−0.56).

2.2.2. *Differences and similarities in networks recruited by task stages*

In this part, we report results on similarities and differences of activation patterns during component phases of the decision-making process. Specifically, we isolated networks of brain structures responsible for financial decisions under risk during decision, anticipation and outcome phases and investigated temporal dynamics and spatial overlap between activations in each of these phases.

2.2.2.1. Decision phase. The decision-making network, showing increased activity as a function of relative behavioral risk, consisted of anterior cingulate cortex, superior frontal gyrus, right posterior cingulate cortex, caudate nucleus, substantia nigra, as well as precuneus, middle occipital gyrus, parahippocampal gyrus and fusiform gyrus (Fig. 3A). Activation patterns reflected in time series not only show an initial peak during choice, but also a second peak during the outcome period for all areas shown in Fig. 3B. This indicates an involvement of these areas in processing outcome-related information, i.e. whether a decision resulted in winning or losing. However, these areas no longer distinguish between selected risk-level during the outcome phase, as expected

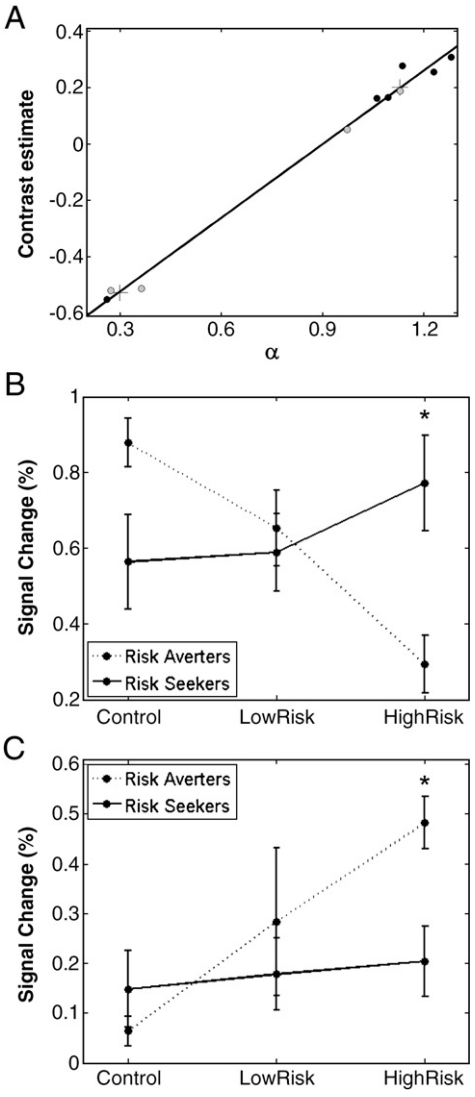

Fig. 5 – Differential brain responses for risk averters and risk seekers. (A) Results from cluster analysis conducted on mean network activity and risk preference (*α*) for each subject. Crosses show centroids for risk averters (bottom left) and risk seekers (top right). Grey data points represent subjects from the BrU sample, black data points represent subjects from the IU sample. (B) Activity in the network of structures showing positive correlations between BOLD responses during risky choice and risk preferences (outlined in Table 3). Risk seekers exhibit an increase in activation as a function of risky choice, while risk averters show a decrease in activation. (C) Activity in the caudate nucleus shows the opposite activation pattern with a decrease as a function of risk for risk seekers and an increase for risk averters. Error bars represent standard error of the mean; "*" denotes significant differences between risk seekers and risk averters.

from this phase constituting a resolution of whether risky choice paid off or not. Additionally, for the PCC and to some extent the SFG, a somewhat sustained response during the anticipation period can be observed that maintains the order of risk-level selected during choice. This result is supported by the finding that an adjacent region of the PCC encodes risk-level during anticipation, implicating this area not only in the selection of risky lotteries, but also in the anticipation of resulting outcomes.

2.2.2.2. *Anticipation phase.* During anticipation, areas that encoded risk-level of choice include the anterior cingulate cortex, posterior cingulate cortex, inferior parietal lobe, inferior temporal gyrus and globus pallidus extending into putamen (Fig. 6A, Table 4). Activation patterns within these regions are shown in Fig. 6B and indicate that these areas are involved in anticipating the outcome of choices with differing relative behavioral risk. All of these areas show increased activations as a function of risk during the anticipation period, as demonstrated by deconvolved time courses and supported by trend analyses of mean peak activations shown in Fig. 6C. Trend analyses yielded the following results for: posterior cingulate cortex [$F(1,8)=34.408$, $p<0.001$, $\eta^2=0.775$], left anterior cingulate cortex [$F(1,8)=17.352$, $p<0.005$, $\eta^2=0.684$], right anterior cingulate cortex [$F(1,8)=19.605$, $p<0.005$, $\eta^2=0.71$], inferior parietal lobule [$F(1,8)=27.549$, $p<0.001$, $\eta^2=0.775$], globus pallidus [$F(1,8)=14.095$, $p<0.007$, $\eta^2=0.638$], and inferior temporal lobe [$F(1,8)=78.629$, $p<0.001$, $\eta^2=0.908$]. These findings were supported by ROI analyses of the parametric effects of risk during anticipation, which indicate that mean regression coefficients were significantly greater than zero in all regions (Table 4).

As done for the decision phase, we also investigated the effect of scanning environment on these activation patterns. Significant effects of scanning environment were found within left and right anterior cingulate cortex, globus pallidus, and inferior temporal lobe. Specifically, a significant interaction between CHOICE and SESSION was observed in both left and right anterior cingulate cortex [left ACC: $F(1,8)=13.092$, $p<0.007$, $\eta^2=0.621$; right ACC: $F(1,8)=13.607$, $p<0.007$, $\eta^2=0.63$], indicating different activation trends within different scanning environments. As done for the decision phase, we performed separate linear trend analyses on our two samples and found a significant linear trend for the IU sample in both areas [left ACC: $F(1,5)=32.436$, $p<0.005$, $\eta^2=0.866$; right ACC: $F(1,5)=56.143$, $p<0.001$, $\eta^2=0.918$], while the BrU sample did not show a significant linear trend [left ACC: $F(1,3)=0.173$, $p=0.705$, $\eta^2=0.055$; Means: CO: −0.013,LR: 0.000, HR: −0.003; right ACC: $F(1,3)=0.157$, $p=0.718$, $\eta^2=0.050$; Means: CO: −0.008, LR: −0.024, HR: 0.002]. Near-significant interactions between CHOICE and SESSION were obtained in globus pallidus and inferior temporal lobe [GP: $F(1,8)=8.46$, $p=0.02$, $\eta^2=0.514$; ITL $F(1,8)=8.766$, $p=0.018$, $\eta^2=0.523$]. Separate linear trend analyses were conducted for our two samples, results of which indicated a significant linear trend for the IU sample in both areas [GP: $F(1,5)=137.409$, $p<0.001$, $\eta^2=0.965$; ITL $F(1,5)=56.813$, $p<0.001$, $\eta^2=0.919$], while, for the BrU sample, this trend persisted in the ITL at near-significant levels [$F(1,3)=21.758$, $p=0.013$, $\eta^2=0.906$; Means: CO: −0.38 LR: 0.10 HR: 0.86], but not in the GP [$F(1,3)=0.128$, $p=0.774$, $\eta^2=0.041$; Means: CO: −0.36, LR: −0.008, HR: −0.19]. Finally, a significant main effect of SESSION was observed in the GP [$F(1,8)=16.143$, $p=0.007$, $\eta^2=0.669$], with greater mean activation in the IU sample (0.113) compared to the BrU sample (−0.21). As mentioned above, one explanation for these minor differences in activation trends in IU and BrU samples is the presence of an equal amount of risk-seeking and risk-averse individuals

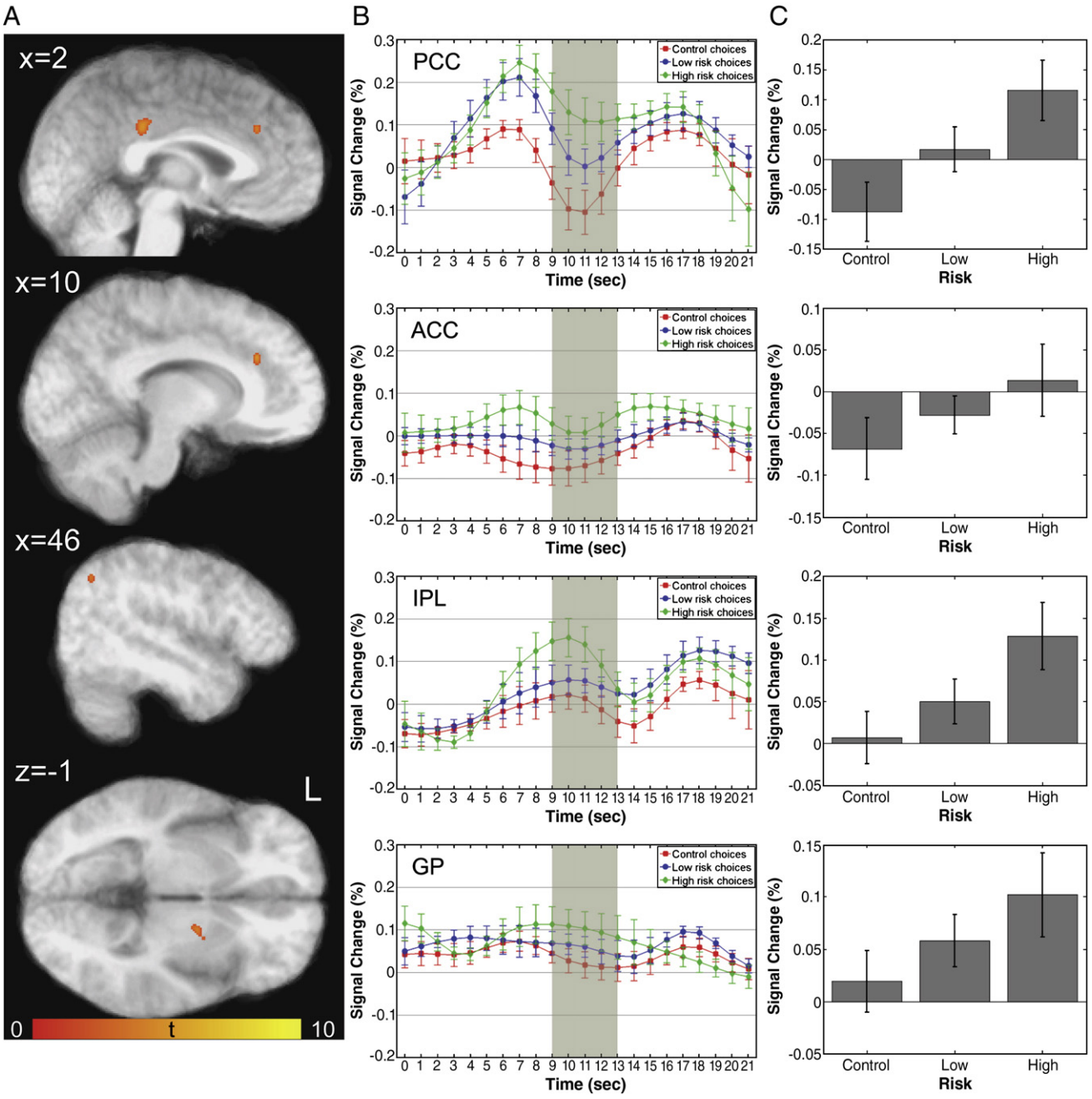

Fig. 6 – Neural correlates of risky choice during the anticipation phase: (A) Plots show regions with activations during the anticipation phase of the task that were significantly modulated by relative behavioral risk associated with subjects choices (high-risk, low-risk, or control). Regions with significant activation during the anticipation period after a risky choice included the posterior cingulate (PCC), anterior cingulate (ACC), inferior parietal lobule (IPL), and globus pallidus (GP). For a complete list of regions showing risk-related modulation during anticipation, see Table 4. (B) Timeseries of activations for each type of decision (high-risk, low-risk, or control), for four regions, PCC, ACC (averaged across two adjacent clusters in left and right hemisphere), IPL, and GP. All regions show risk-modulated neural activity that is maintained throughout the anticipation period. (C) Mean peak activations in each of the regions represented in (B). All regions illustrate a significant linear trend of increased activation with increased relative behavioral risk.

in the BrU sample, which show opposite activation patterns that may average out. Taken together, these findings indicate that differences in scanning environments had an effect on activation trends within a subset of areas activated during the anticipation phase in the current study, i.e. ACC and globus pallidus, indicating that within these areas, trends were driven mostly by the more risk-seeking IU sample.

Deconvolved time courses within the PCC, shown in Fig. 6B, show that after an early peak during the decision phase, activation is maintained during the anticipation phase such

Table 4 – Areas showing significant activation during the anticipation period after a risky choice was made.

Structure	L/R	BA	Volume	X	Y	Z	Max T	Parametric effects	
								$Mean_{slope}$	T_{slope}
Superior frontal gyrus	R	10	81	30.6	44.6	2.5	6.6453	0.0016	4.3927***
Anterior cingulate cortex	R	32	108	9.1	31.5	26.8	8.9699	0.0049	6.9749****
Anterior cingulate cortex	L	9	135	−3.8	30.4	31.8	6.0111	0.0073	5.0675****
Globus pallidus/putamen	R		216	19.1	−0.8	0.2	5.9744	0.0032	2.9793*
Inferior temporal gyrus	R	20	189	53.5	−25.1	−13.7	7.8561	0.0045	3.6343**
Posterior cingulate cortex	L	31	324	−2.3	−32.2	33	6.4806	0.0125	5.4475****
Inferior parietal lobule	R	39	108	46.5	−62.3	37.8	5.3131	0.0162	4.0562***

Volume (in μl), Talairarch coordinates of activation peaks, and results from ROI analyses of the parametric effects of risk (mean slope as well as significance level) are also shown.
n.s.: near-significant; *: significant at $p<0.05$; **: significant at $p<0.01$; ***: significant at $p<0.005$; **** significant at $p<0.001$.

that activation increases linearly as a function of relative behavioral risk during this period. A slight peak can be observed during the outcome phase during which relative ordering of chosen risk-level is maintained. This indicates that the PCC is involved in all stages of the decision-making task employed in the current experiment. However, in the area of the PCC that activates maximally during anticipation (Fig. 6A), distinction between risk-level occurs only from late decision till early outcome periods and is at its peak during anticipation, implicating this subregion of the PCC mainly in reward anticipation. A similar time course can be observed in the ACC, whose activation patterns show two peaks during decision and outcome periods and maintain distinction between risk-level of choice during the anticipation period. Of note, subregions of ACC and PCC shown here are adjacent to, and show some overlap with, activation clusters obtained during the decision period, as illustrated in Fig. 8. The inferior parietal lobule shows an activation pattern indicative of its involvement primarily in anticipation and outcome periods. Activation that increases with relative behavioral risk during anticipation can be observed, indicating that this area risk during the anticipation period. This is no longer the case during the outcome period. Finally, the time course of the globus pallidus follows a similar pattern during the anticipation period only, showing increased activations as a function of relative behavioral risk.

2.2.2.3. Outcome phase. In agreement with previous research (e.g. Knutson et al., 2001b; Tricomi et al., 2004; Zink et al., 2004), the contrast of winning versus losing revealed enhanced activations after winning in a wide network of structures including, but not limited to, striatal areas typically associated with reward processing such as left ventral striatum (including nucleus accumbens), bilateral caudate nucleus and putamen, frontal areas such as ventral and middle anterior cingulate cortex, middle frontal gyrus (BA10), and posterior cingulate cortex, and due to the visual nature of this phase of the task, bilateral lingual gyrus and left occipital gyrus, as well as attentional areas including frontal eye fields, superior parietal lobule, inferior parietal lobule and precuneus (Fig. 7A) (Table 5). Time courses within a subset of these areas are shown in Fig. 7B and demonstrate increased activations after winning compared to losing during the expected peak in the outcome phase. Mixed ANOVAs were conducted to investigate the increase in activations after winning compared to losing and, additionally, potential effects of scanning environment. Significantly greater BOLD responses after winning compared to losing were obtained in the following areas shown in Fig. 7C: ventral ACC [$F(1,8)=209.094$, $p<0.001$, $\eta^2=0.963$], PCC [anterior: $F(1,8)=46.659$, $p<0.001$, $\eta^2=0.854$; posterior: $F(1,8)=92.146$, $p<0.001$, $\eta^2=0.92$], ventral striatum [$F(1,8)=30.546$, $p<0.001$, $\eta^2=0.793$], and frontal eye fields [$F(1,8)=19.655$, $p<0.005$, $\eta^2=0.711$], with a near-significant effect in middle ACC [$F(1,8)=5.796$, $p=0.043$, $\eta^2=0.420$]. Significant effects of scanning environment were found within ventral anterior cingulate cortex and ventral striatum as indicated by a significant interaction between OUTCOME and SESSION in vACC: [$F(1,8)=43.717$, $p<0.001$, $\eta^2=0.845$] and a near-significant interaction in vSTR [$F(1,8)=9.695$, $p=0.014$, $\eta^2=0.548$]. As done for the previous two phases, we further investigated these effects by conducting separate tests for each of the samples. Pairwise *t*-tests indicated a significant increase in activation after winning in ventral ACC for the IU sample and a near-significant increase for the BrU sample [IU: $t(5)=24.731$, $p<0.001$; BrU: $t(3)=3.665$, $p=0.35$], but only for the IU sample in ventral striatum [IU: $t(5)=7.560$, $p<0.001$; BrU: $t(3)=1.364$, $p=0.266$]. It has to be noted, however, that BOLD responses in both regions followed the expected trend, with greater responses after winning compared to losing [vACC: won=−0.026, lost=−0.072; vSTR: won=0.41, lost=−0.006]. Taken together, these findings indicate that differences in scanning environments had a negligible effect on activation trends during the outcome phase in the current study.

Patterns apparent in deconvolved time courses within PCC and ACC show little involvement during other phases as a function of winning, while vSTR and FEF show additional peaks during the decision period. Interestingly, when subjects lost, large increases in activation after termination of the outcome phase can be observed in PCC and FEF. These increases occur just before the onset of the next trial and may therefore indicate a preparatory attentional signal in FEF and PCC that is influenced by the affective salience of having lost on the current trial.

2.2.2.4. Areas of overlap between task phases. The temporal 'overlap' between phases apparent in time courses shown in Figs. 3B, 6B and 7B indicated that some areas, particularly ACC, PCC and caudate nucleus, were recruited during multiple phases of our decision-making task. This raises the question to what extent these areas overlap spatially. To further investigate the relative involvement of these areas in different phases of the decision-making task employed in the current

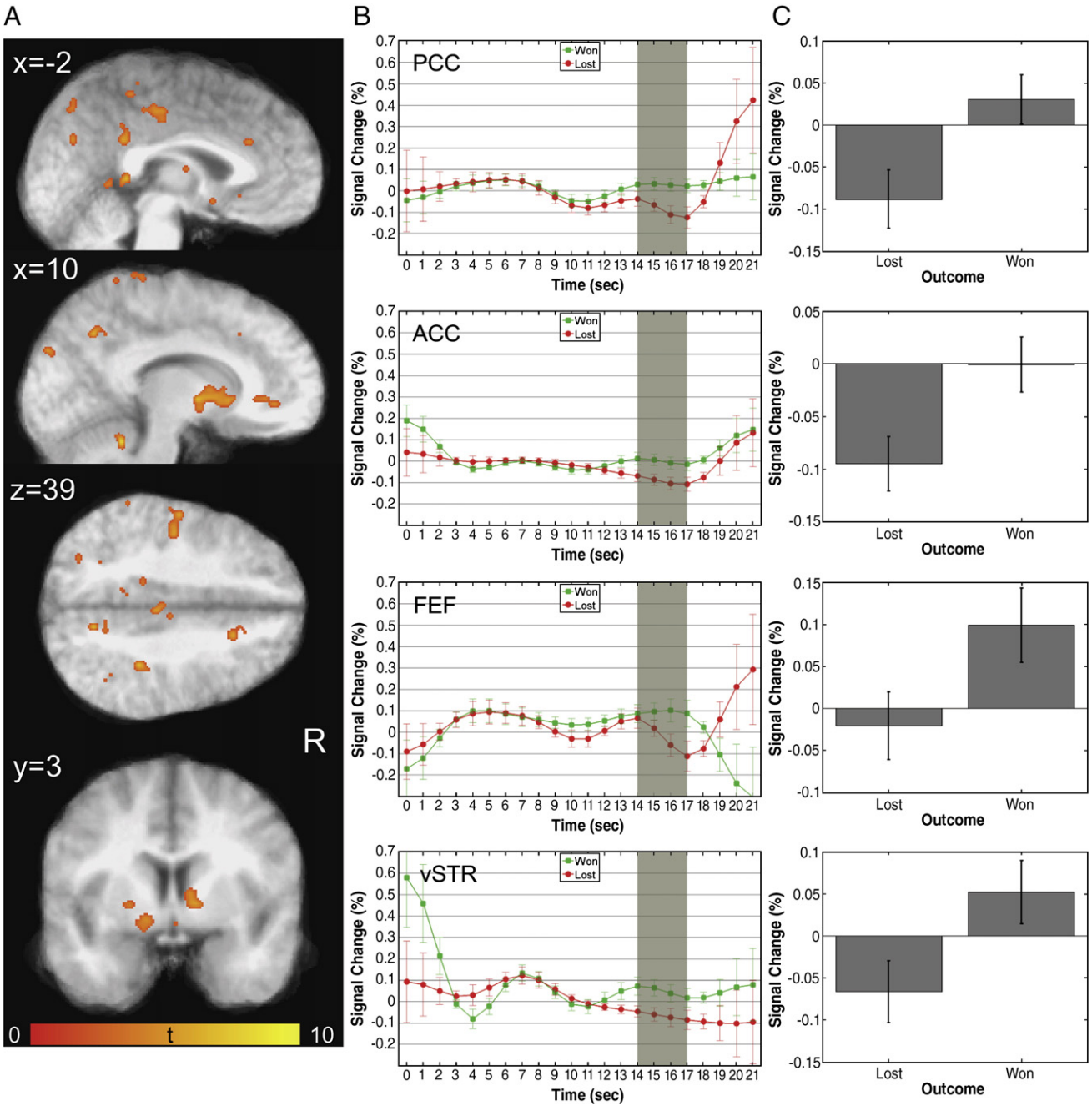

Fig. 7 – Outcome Phase: (A) Plots show regions significantly more active during the outcome phase for trials where the subject is informed of a win versus a loss. A diverse network of structures showed significant outcome-related modulation of activity during this phase of the task. A subset of regions, including PCC, ACC, frontal eye fields (FEF), ventral striatum (vSTR), and caudate are shown here. For a complete list of regions showing outcome-related, see Table 5. (B) Timeseries of neural activity for outcomes of wins (green) and losses (red) in four regions: PCC (average of two clusters), ACC, FEF, and vSTR. In region shown here, timeseries for wins and losses maintain a similar course prior to the outcome presentation, at which point they diverge into relative increases and decreases of activation for wins and losses, respectively. (C) Mean peak activations in each of the regions represented in (B). Each region showed significantly greater BOLD responses following wins.

experiment, we compared activations exhibited during each of the task phases with those of all other task phases using conjunction analysis (Fig. 8, activations during each phase thresholded at $p=0.01$ are shown in the following colors: decision: *red*, anticipation: *green*, outcome: *blue*, overlap between task phases is illustrated by blending these colors, see SM Table 2 for extent and coordinates of overlap). As expected from time-series analyses, regions of overlap

Table 5 – Areas showing significant activation during the outcome period after (won vs. lost).

Region	L/R	BA	Volume	X	Y	Z	Max T
Anterior cingulate cortex	L	32	405	−10.8	35.9	0.1	10.559
Anterior cingulate cortex	L	32	135	−0.9	27.4	25.9	6.7835
Anterior cingulate cortex	R	24	2781	7.4	21.9	1.8	10.449
Caudate/putamen	L		918	−17.1	5.1	−0.7	9.8733
Precentral gyrus	L	4	351	−58.3	−7.5	20.6	10.187
Precentral gyrus	R	4	243	56.9	−10.6	21.5	9.6081
Frontal eye fields/precentral gyrus	L	4	594	−48.7	−12.9	37.4	8.4102
Caudate body	L		270	−16.2	−17.8	21.2	7.4139
Postcentral gyrus	L	3	216	−34	−20.7	46.6	7.329
Postcentral gyrus	R	2	135	47	−20.9	28.4	8.1057
Posterior Cingulate (mid)	Bi	31	864	−1	−21.7	41.6	7.7431
Caudate nucleus	R		162	18	−23.5	25.5	6.2724
Inferior parietal lobe	R	40	162	32.8	−32.6	38.9	8.8703
Paracentral lobe	R	6	216	2.3	−33.1	61.7	6.945
Inferior parietal lobe	L	40	189	−32.4	−40.5	50.5	5.374
Posterior cingulate (posterior)	L	31	621	−5.7	−41.4	30.9	7.7569
Cerebellum	L		513	−42.1	−44.3	−31.6	9.1656
Posterior cingulate	Bi	29	972	−2.7	−45.2	5.5	10.602
Cerebellum	L		378	−14.8	−46.9	−38.5	8.3562
Cerebellum	R		162	42.5	−47.5	−37	5.7249
Cerebellum	L		405	−28.7	−50.4	−51.8	7.6883
Superior parietal lobe	R	7	189	30.3	−54.9	55.8	6.6982
Precuneus	R	7	189	10.5	−56.3	39.4	9.8227
Cerebellum	R		135	44.8	−57.4	−41.9	6.4334
Cerebellum	R		135	20.1	−57.4	−28.1	7.3549
Cerebellum	L		756	−37.1	−58.9	−34.8	10.778
Precuneus	L	39	243	−27	−58.9	33.4	8.6662
Fusiform gyrus	L	37	216	−38.8	−59.2	−17.8	9.2095
Cerebellum	L		351	−27.4	−64.5	−22.1	6.7936
Cerebellum	Bi		729	−3.2	−64.6	−38.9	8.104
Cuneus/precuneus	L	31	648	−18.5	−64.6	21.3	7.6699
Middle temporal gyrus	R	39	216	35.7	−66	21.9	6.3188
Superior parietal lobe	L	19	216	−28.2	−67	40.1	6.5363
Lingual gyrus	L	18	432	−15.9	−70.3	−7.9	6.8375
Mid occipital gyrus	R	19	270	45.2	−70.5	−9.3	7.1198
Precuneus	Bi	7	162	−0.5	−71	46.5	6.1356
Precuneus	L	31	270	−4.7	−71.4	28.9	6.5932
Mid occipital gyrus	L	19	162	−35	−83	17	7.5394
Cuneus	R	19	189	10.2	−84.2	29.2	7.3955
Superior occipital gyrus	R	19	243	23.2	−85.6	28.2	6.0963
Inferior occipital gyrus	R	18	459	27.7	−89.7	−3.6	7.0199

Volume (in μl) and Talairarch coordinates of activation peaks are also shown.

included the anterior and posterior cingulate cortices, which showed significant activations throughout all task phases, as well as the caudate nucleus. The largest overlap between ACC and PCC was observed in comparisons of decision with anticipation periods (Fig. 8A). Additional overlap was observed in the thalamus and right caudate. When comparing activations during anticipation and outcome periods, overlap was also found in ACC and PCC, and, additionally, in the right caudate nucleus (Fig. 8B). Finally, decision and outcome periods showed overlap in PCC and two regions of ACC (middle and ventral), as well as left caudate, right ventral striatum and cuneus and precuneus. These findings indicate that, at a threshold of $p=0.01$, there was considerable overlap between a subset of areas active during different task phases, particularly in the anterior and posterior cingulate cortex and with less consistency, the caudate nucleus. The extent of this overlap was decreased to a few voxels in ACC, PCC and caudate when the threshold was lowered to $p=0.001$ (Fig. 8D). Taken together, these findings indicate that a subset of areas is recruited throughout all task phases. These areas, however, interact with different regions that are recruited exclusively during each of the task phases.

3. Discussion

In the current study, we investigated the neural correlates of subjective valuations during financial choice. Participants chose between lottery pairs of identical expected value, but with varying levels of risk and reward, offering a choice between a lottery yielding a higher payoff at a comparatively large risk or a competing lottery yielding a lower payoff but involving less risk. Since expected value was constant across all lotteries, decisions were mainly influenced by participants' risk preferences. Behavioral results revealed a continuum of risk attitudes that ranged from risk-seeking to risk-averse.

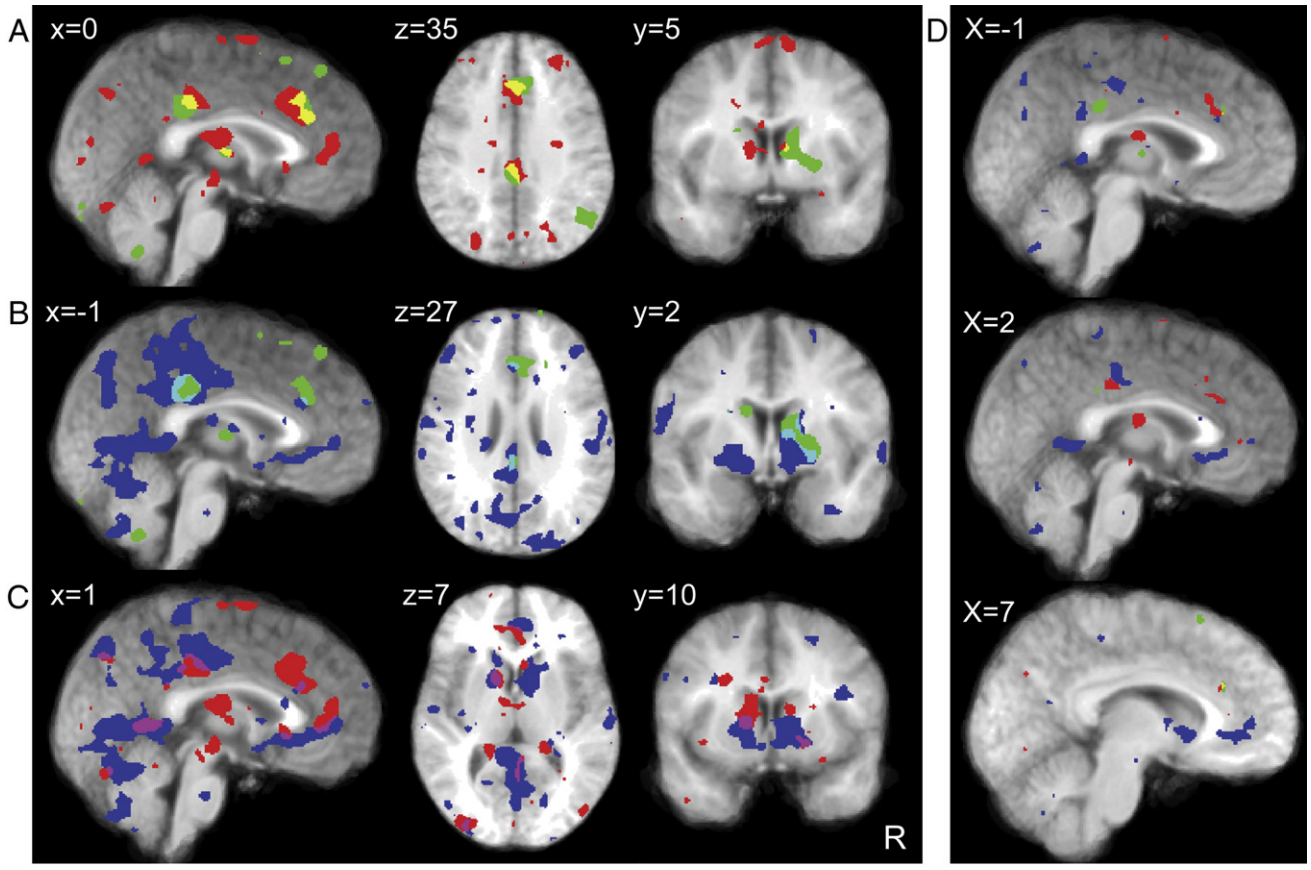

Fig. 8 – Activations across all task phases: Conjunction maps in A–C illustrate the overlap of regions significantly active ($p<0.01$) in each of the task phases. Though the networks are largely distinct, overlap is consistently found in regions of the ACC, PCC, and caudate nucleus, and, to a lesser extent, in thalamus, ventral striatum, cuneus, and precuneus. (A) Regions of overlap (yellow) between areas activated during decision-making (red) and anticipation (green) phases. (B) Regions of overlap (turquoise) between areas activated during anticipation (green) and outcome (blue) phases. (C) Regions of overlap (pink) between areas activated during decision (red) and outcome (blue) phases. (D) Overlap remains in ACC, PCC and caudate at $p<0.001$.

Brain signals revealed that activity in a set of regions previously associated with risky choice showed increased activity when subjects chose options with greater relative behavioral risk. Furthermore, responses during choice were modulated by participants' risk preferences and a network of structures showed activation patterns that maximally differentiated between risk-averse and risk-neutral participants. These findings underline the importance of subjective factors during financial choice, leading to heterogeneous risk preferences that significantly impact brain responses during choice.

3.1. *Neural correlates of risk preference during choice*

Participants' risk attitudes, extracted from choices made on using nonlinear logistic regression, varied between risk-averse and mildly risk-seeking preferences. The heterogeneity in risk preferences evident in the current behavioral results not only agrees with previous findings from neuroimaging and behavioral experiments (e.g. Fetherstonhaugh et al., 1997; Huettel et al., 2006; Kable and Glimcher, 2007; Schunk and Betsch, 2006), but underlines the importance of subjective factors in decision-making. To investigate how risk preferences expressed during choice manifest neurally, we probed for areas that encode relative behavioral risk during choice, such that increased risk-level in participant's choices was associated with a parallel linear increase in BOLD activity of structures within this network. Activation patterns apparent in deconvolved time series showed such increased BOLD responses as a function of relative behavioral risk, which was supported by trend and parametric ROI analyses, in a network that included regions typically associated with conflict monitoring, such as the anterior cingulate cortex, task control and selection of action sets, such as the superior frontal gyrus and posterior cingulate cortex, reward processing, such as the caudate nucleus and an area in the brainstem that is consistent with the substantia nigra, as well as visual and attentional areas such as precuneus, middle occipital gyrus, parahippocampal gyrus and fusiform gyrus. These findings confirm results from previous studies implicating similar networks in risky decision-making (Ernst et al., 2004; Eshel et al., 2007; Huettel, 2006; Huettel et al., 2005; Paulus et al., 2001, 2005; Paulus and Frank, 2006; Rogers et al., 1999, 2004;

Tobler et al., 2007). Our results extend previous research by suggesting a fundamental role of these nodes in representing risk preference during economic decision-making in an experimental setting that emphasized *subjective* valuations during choice. Furthermore, our activation maps show overlap with a network of structures implicated in processing subjective value during intertemporal choice in a recent study, including medial prefrontal cortex, posterior cingulate cortex and striatum (Kable and Glimcher, 2007). The current results extend these findings by demonstrating that risk preferences revealed during decision-making under risk are processed in a similar network during a task not involving intertemporal choice.

We furthermore investigated whether individual differences in risk attitude modulated activations during risky decision-making. To obtain an estimate of participants' risk attitude, we extracted the curvature of the utility function from choices made during scanning using nonlinear logistic regression. We regressed this parameter against activity showing a linear increase in activity as a function of relative behavioral risk during choice. Significant correlations with activations during risky decision-making were obtained in a network partially overlapping with the network involved in risky choice described above, including IFG, SFG, medial OFC, bilateral OFC/VLPFC (BA47) and caudate nucleus. Additional regions showing significant modulation by risk preference during decision-making included hippocampus, parahippocampal gyrus, putamen and lingual gyrus. All regions within this network, with the exception of the caudate, showed a positive correlation with behavioral risk preference, indicating that increased activity within this network during risky choice predicted participants' propensity to take higher risks for larger payoffs. These results demonstrate that activity in structures previously implicated in risk-taking behavior (e.g. Ernst et al., 2004; Eshel et al., 2007; Huettel, 2006; Rogers et al., 1999, 2004; Tobler et al., 2007; Vorhold et al., 2007) was modulated by risk attitude. In particular, our results demonstrate increased activations as a function of relative behavioral risk in this network of structures when risk-seeking individuals made risky choices, while activity decreased when risk-averse individuals made risky choices (Fig. 5B). The network of structures modulated by individual differences in risk attitude showed significant overlap with circuits previously implicated in cognitive control, response inhibition and cognitive flexibility (IFG, BA47, SFG) (Bush et al., 2002; Casey et al., 2001; Nagahama et al., 1999; O'Doherty et al., 2003a; Tanaka et al., 2008). Increased activations in participants expressing risk-neutral to mildly risk-seeking behavior were observed in these regions, suggesting increased engagement of cognitive control processes. Interestingly, a risk-seeking choice strategy could lead to the highest potential total gain in the context of the current experiment. This strategy may therefore be the preferred approach for "deliberate" decision-makers and may require successful suppression of negative anticipatory emotions in order to maximize gain (Schunk and Betsch, 2006). In accordance with this interpretation, increased activation in this network may be related to increased employment of cognitive control and emotion regulation strategies, as previously shown (Delgado et al., 2008; Ochsner et al., 2004a,b).

Significant negative modulations of neural responses during risky choice by behavioral risk preference, on the other hand, were obtained in the right caudate nucleus. This result demonstrates increased activation as a function of selected risk-level when risk-averse individuals engaged in risky choice and shows the opposite activation pattern for risk-seeking individuals (Fig. 5C). The caudate nucleus is typically thought to be involved in reward-related processing (e.g. Delgado et al., 2005a,b; Delgado et al., 2004; Tricomi et al., 2004; Zink et al., 2003, 2004). Increased activity in this area may therefore be related to increased payoff magnitude, which, in the current study, was coupled with increased risk. Activity in the caudate nucleus may signal to risk-averse subjects that it may be worthwhile to take a risky option that is linked to a large potential payoff. We therefore tentatively suggest that, for risk-averse individuals to engage in risky decisions, activity in the caudate may need to exceed a certain threshold to override conservative default behaviors apparent in these individuals, which may be suppressed by engagement of emotion regulation strategies in risk-seeking individuals. Taken together, these results suggest that individual differences in risk attitude may be driven by differences in decision strategies, with risk-averse individuals basing choices mainly on affect, while risk-neutral individuals employ a more cognitive strategy that maximizes potential rewards.

Various prior studies have investigated individual differences in behavioral risk preference. Paulus et al. (2003) have demonstrated that activation in the anterior insula was related to participants' propensity to select a safe response following a punished response as well as participants' degree of neuroticism and harm avoidance, and, in a more recent study, intolerance to uncertainty (Simmons et al., 2008). Furthermore, an area in the anterior cingulate has been shown to correlate with the degree to which participants were risk-seeking for low probability prospects and risk-averse for high probability prospects (Paulus and Frank, 2006). Finally, activation in the ventral striatum has been shown to correlate with behavioral loss aversion (Tom et al., 2007). A recent study by Tobler et al. (2007) showed that neural activations in two clusters within the orbitofrontal cortex distinguished risk seekers, as demonstrated by negative correlations with risk-aversion in medial OFC, from risk-averse individuals, as demonstrated by a positive correlation with risk-aversion in right lateral OFC. In the context of the current experiment, two networks distinguish between risk-averse and risk-neutral individuals. Specifically, positive correlations with risk-seeking attitudes were obtained in both bilateral and medial OFC and an extended network consisting of IFG, SFG, parahippocampal gyrus, putamen and lingual gyrus, while caudate nucleus, and to a lesser extent, anterior insula, correlated with risk-averse attitudes.

3.1.1. *Neural correlates of risk preference during anticipation*

To investigate how subjective preferences expressed during choice affect activations during the anticipation period, we probed for areas encoding risk-level of choice during this task phase. In accordance with results from the decision period, activation patterns apparent in deconvolved time series showed increased BOLD responses as a function of riskiness, which was supported by trend and parametric analyses, in a

network of structures that included the anterior cingulate cortex, posterior cingulate cortex, inferior parietal lobe, globus pallidus extending into putamen and inferior temporal gyrus. These results agree with findings from previous research, which demonstrated activations during the delay period of a decision-making task involving risk in medial prefrontal cortex, inferior parietal lobe and inferior frontal gyrus (Critchley et al., 2001). Here we confirm results from prior studies by showing that risk modulates activity in ACC during anticipation. Our results also show that risk-modulated activity in a distributed network of areas involved in anticipating potential gains including PCC, IPL and GP. This relative increase in network size in comparison to previous research may be due to the fact that, in the current study, subjects' choices directly affected risk-level and gain magnitude leading to increased control over obtaining a monetary outcome. Such response-contingency may lead to wider activations, as demonstrated for the caudate nucleus previously (Tricomi et al., 2004), particularly in areas involved in attention (IPL), affect (PCC), as well as reward expectation (GP) during this task phase (see also McCoy and Platt, 2005; Platt and Glimcher, 1999).

A consistent result in both animal electrophysiology and human functional neuroimaging studies is the activation of ventral striatum, particularly nucleus accumbens, during the anticipation of rewarding outcomes (Breiter et al., 2001; Knutson et al., 2001a,b, 2003, 2007). This finding was not replicated in the current experiment. The reason why we did not observe significant activations in ventral striatum during anticipation of gains in the current study may be due to task differences, as well as differences in statistical models of responses during the anticipation period, which probed for areas encoding riskiness selected during the decision period in the current experiment. One task that has consistently demonstrated significant BOLD responses in the nucleus accumbens is the monetary incentive delay task (MID), in a version of which subjects view a brief cue indicative of amount and probability of winning, wait for the duration of a delay, after which they are asked to respond to a brief target. Finally, subjects receive feedback indicating how much money was won or lost on a given trial (Knutson et al., 2001a,b, 2003; for a review see Knutson and Peterson (2005)). While the outcome in the MID task is response-dependent, the response occurs after the anticipation period and, importantly, does not determine probability or magnitude of potential outcomes on a given trial. The task employed in the current study required participants to make a selection between lotteries of differing risk-levels/outcome magnitudes before anticipation, to allow participants to express their preferences for a particular lottery. Importantly, neural responses during anticipation were modeled in terms of risk-level selected during choice and not in terms of the expected reward. Also of note, activations during this period were not driven by unpredictability in the current experiment (e.g. Berns et al., 2001; Knutson et al., 2001a), because activations were modeled in terms of selected risk-level of lottery pairs involving equal levels of unpredictability (e.g. 40% vs. 60%; 90% vs. 10%). In this context, it appears that a separate area in striatum encodes preferred risk-level/reward magnitude selected during choice, namely globus pallidus. This interpretation is consistent with previous research implicating this structure in coding reward-related behaviors and reward expectation in both animal electrophysiology (Arkadir et al., 2004; McAlonan et al., 1993; Schultz et al., 1992) and human neuroimaging studies (Aron et al., 2005; Elliott et al., 2000; Menon et al., 2007).

3.1.2. *Outcome related brain signals*

During the outcome phase, participants were informed about whether they won or lost. This phase constitutes a resolution of whether relative behavioral risk selected during the decision phase paid off and was therefore modeled in terms of winning versus losing. Significant activations showing increased BOLD responses after wining were obtained in a wide network of structures including, as expected, areas previously implicated in computing the reward prediction error, such as left ventral striatum (including nucleus accumbens), bilateral caudate nucleus and putamen. Furthermore, we found activations in frontal areas, such as ventral and middle anterior cingulate cortex extending into medial orbitofrontal cortex, middle frontal gyrus (BA10), and posterior cingulate cortex, and due to the visual nature of this phase of the task, bilateral lingual gyrus and left occipital gyrus, as well as attentional areas including frontal eye fields, superior parietal lobule, inferior parietal lobule and precuneus. These findings are largely in agreement with previous research (e.g. Knutson et al., 2001b, 2003; Knutson and Peterson 2005; McClure et al., 2003; Menon et al., 2007; O'Doherty et al., 2003b; Tricomi et al., 2004; Zink et al., 2004).

3.1.3. *Similarities and differences in activation patterns during different task phases*

In order to investigate the potential involvement of regions showing significant BOLD activations during a particular task phase across multiple task phases, we conducted time course analyses. Time courses not only demonstrated increased responses as a function of risk during expected peak responses in decision and anticipation phases, but also showed that a subset of areas within each phase were involved in processing events in other phases. This observation was particularly consistent for the posterior (PCC) and anterior cingulate cortex (ACC), which both showed involvement during choice, followed by maintenance of activity reflecting risk during anticipation, and, finally, a second peak during the outcome phase. These findings are corroborated by conjunction maps showing spatial overlap between activation clusters in ACC and PCC, and, the caudate nucleus. This overlap was consistent across all task phases.

These findings indicate that a subset of adjacent and partially overlapping areas, particularly in ACC and PCC, is recruited throughout all trial phases and interact with different regions that are recruited exclusively during each of the task phases. While previous research has dissociated different phases of reward processing (e.g. Liu et al., 2007; for review see also Knutson and Cooper (2005)), to our knowledge, this is the first study on decision-making demonstrating that adjacent and overlapping areas of ACC, PCC and caudate nucleus are involved in all task phases, as evident from both time course and conjunction analyses. We suggest a role of these areas in self-referential subjective valuations that entail cognitive and affective components and persist

throughout all task phases. Specifically, due to the involvement of ACC in conflict and performance monitoring (e.g. Bush et al., 2000, 2002; Kerns et al., 2004; Krawczyk, 2002; Ridderinkhof et al., 2004), this area may be involved in mediating cognitive components of subjective valuations involving risk. Interestingly, an adjacent area in medial prefrontal cortex has previously been shown to be involved in self-referential states (Castelli et al., 2000; Gusnard et al., 2001). The PCC, on the other hand, has been implicated in emotional processing (e.g. Chandrasekhar et al., 2008; Maddock et al., 2003; Small et al., 2001; Vogt et al., 2003; for reviews see Maddock (1999) and Vogt et al. (2006)), self-reflection and self-imagery (Johnson et al., 2002; Kircher et al., 2001, 2002; Phan et al., 2004; Sugiura et al., 2005, 2006), as well as being part of a default network thought to involve self-referential internal dialog (Gusnard and Raichle, 2001). We therefore suggest that this area may be involved in mediating affective components of subjective valuations involving risk. This interpretation is consistent with previous research implicating these structures in (1) tracking subjective value of delayed monetary rewards (Kable and Glimcher, 2007), (2) mediating internal goals and processing self-referential mental activity as part of a default cortical system (Castelli et al., 2000; Gusnard and Raichle, 2001; Shulman et al., 1997; Zysset et al., 2002); and (3) encoding probability and reward size in both reinforcement learning tasks, choice tasks and attention tasks (e.g. Knutson et al., 2005; Kuhnen and Knutson, 2005; McCoy et al., 2003; Rogers et al., 2004; Small et al., 2005). Of note, our findings are also in accordance with a conclusion from a recent review of the monkey electrophysiology and human neuroimaging literature on the neuroeconomics of risky decision-making (Platt and Huettel, 2008), which stated that the posterior cingulate cortex plays and evaluative role during decision-making, linking external events and actions to subjective psychological states.

3.1.4. *Limitations of the present research*

A few issues should be noted before accepting any strong interpretations of our results. First, the data were collected from two smaller subsets of subjects at separate imaging sites. The variance added by using data from multiple sites makes our design suboptimal as it decreases power and could lead to problems of underdetection. All analyses accounted for scan site differences accordingly, by including site as a covariate in second-level analyses and as a between-subjects factor in all ROI analyses. To account for magnet signal intensity differences, responses were converted to percent signal change during preprocessing. Differences due to context or task changes were not evident in behavior, and any variations in neuroimaging results between the two samples are noted above. Finally, our conclusions are based on results from multiple independent models (convolved and time-series analyses, as well as linear trend and parametric analyses). The robustness of our effects across these models and their consistency with previous results lends further support to our findings despite reductions in power that may have resulted from collecting data from two scan sites. Second, future studies on individual differences would benefit from including larger sample sizes. Small sample sizes can lead to studies with low power and further compound problems with underdetection (Yarkoni, in press). Furthermore, decreases in power due to the limited sample size can lead to an overestimation of correlation effect sizes (Yarkoni, in press). To address this issue in analyses of the neural correlates of individual differences in risk preference, we employed a bootstrap method with replacement to estimate population correlation coefficients. This method provides a more conservative estimate of correlation coefficients by reducing the influence of potential outliers that might inflate effect size. Means of the resulting distributions of Pearson's ρ remained significant for all but two regions, namely the thalamus and orbitofrontal cortex. Third, because we controlled for expected value in all of our lotteries, the relative behavioral risk of a decision is correlated with reward magnitude and inversely correlated with probability of reward in experimental conditions. In these trials, the highest level of relative behavioral risk was associated with the greatest reward potential, and the lowest probability of reward. Activation patterns as a function of relative behavioral risk during decision and anticipation periods may therefore in part be driven by reward and probability related cognitive processes. This is an unlikely explanation, however, because intermediate risk and reward levels were offered during the control condition, which yielded the lowest activity in all regions of interest during both, decision and anticipation periods. A further alternative explanation for these activation patterns is decision conflict, which is absent in the control condition and may increase as a function of relative behavioral risk. Choosing the option with greater reward at a greater risk may entail enhanced levels of decision conflict and lead to increased activations in relevant regions. However, decision conflict was absent during the anticipation period, which showed similar activation patterns in partially overlapping brain regions. Finally, these confounds play a much smaller role in behavioral analyses, as well as results from individual difference, and parametric analyses, which all support the assertion that relative behavioral risk was the factor driving the reported behavioral and neural responses.

3.1.5. *Conclusions*

In summary, the current study demonstrated that both subjective assessments of risk during choice, as well as individual attitudes toward risk play a significant role in modulating activity in neural networks recruited during decision-making. Specifically, increased relative behavioral risk led to increased activations in a network of structures previously implicated in risky decision-making. Risk attitude, on the other hand, modulated activations during risky choice in a separate, but partially overlapping network that is typically associated with cognitive control processes, as well as caudate nucleus. Activation patterns in this network differentiate between risk-seeking and risk-averse individuals, suggesting that risk-averse and risk-seeking decision-makers employ different decision strategies. Finally, the use of an event-related design allowed us to investigate the dynamics of neural responses relevant to each component task phase using timeseries and conjunction analyses. Though the networks engaged in each of the three task stages were mostly distinct, regions of the ACC, PCC and caudate

nucleus showed consistent temporal and spatial overlap. These results demonstrate the relevance of ACC, PCC and caudate during each phase of a decision-making task that emphasized subjective valuations, strengthening the role of these regions in self-referential subjective valuations during choice, as suggested previously (Kable and Glimcher, 2007; Platt and Huettel, 2008).

4. Experimental procedures

4.1. Participants

Ten right-handed volunteers (7 men and 3 women, 18–31 years; 4 from the Brown University community, 6 from the Indiana University community) participated in the current study, which was approved by the Institutional Review Boards of Brown University, Indiana University and the Memorial Hospital of Rhode Island. Participants reported no psychiatric disorders and had normal or corrected to normal vision.

4.2. Stimuli

Stimuli were pairs of pie charts representing the amount of money that could be won with a particular likelihood (Fig. 1A). The likelihood of winning and not winning each gamble was represented by the size of the slice, with larger areas indicating larger likelihoods. The positive outcome was represented in the green slice together with the respective monetary value in its center, while the negative outcome (not to win any money) was represented in the red slice together with its monetary value ($0). The following reward and probability values were included: (a) 90% probability of winning $2 versus 10% probability of winning $18; (b) 60% probability of gaining $3 versus 40% probability of gaining $4.50; and (c) 50% probability of gaining $3.60 for both lotteries in the control condition. Location of lotteries was counterbalanced across trials. During the outcome phase, only the pie chart of the chosen gamble was displayed with the slice representing the outcome flashing in yellow and the original color (green for winning, red for losing).

4.3. Task

The task consisted of a forced-choice between gamble pairs that reflected different probabilistic monetary outcomes (Fig. 1A). Each trial included a sequence of three phases: (a) a selection phase (3 s), (b) an anticipation phase (6 s) and (c) an outcome phase (3 s). During the selection phase, participants either viewed a gamble pair consisting of one high-risk/reward magnitude choice and one comparably lower risk/reward magnitude choice in the experimental conditions, or they were presented with a choice between two equivalent lotteries reflecting a 50% chance of winning an intermediate reward in the control condition. All lotteries had the same expected value (EV = objective reward magnitude × probability) of 1.8, in order not to bias participants' choices towards one gamble type. Two experimental conditions and one control condition were used in the experiment. Experimental conditions offered participants a choice between an option involving a high risk of gaining a large reward and another option involving a lower risk of obtaining a small reward and thus required an evaluation of the relative increase in risk required to gain a relatively larger reward. Evaluations involving risk and reward magnitude were absent in the control condition as subjects made a selection between two identical lotteries.

Participants were instructed to choose one of the lotteries by pressing one of two buttons assigned to either gamble A (left) or gamble B (right) within 3 s. Failure to do so resulted in losing that particular trial. During the anticipation phase, participants were asked to fixate on a central cross. Finally, during the outcome phase, a computer algorithm determined winnings on a given trial by using the probabilities of the selected lottery in combination with a randomization procedure to toss a virtual, biased coin. The cash amount that was won was then added to a virtual account reflecting cumulative earnings, which was shown to participants together with information about whether they won or lost. Participants were informed of this procedure and that they would receive 5% of their earnings as a final cash reward, which ranged between $10.00 and $20.00.To familiarize participants with the contingencies of the task and minimize learning effects, a brief behavioral training session was completed immediately before the scanning session.

Participants completed either 4 to 5 runs lasting 7.6 min each, or 10 runs lasting 4.2 min each. 7.6 min runs were comprised of 38 12-second trials including 10 High-risk trials, 10 Low-risk trials, 10 Control trials and 8 Null trials during which participants fixated on a central fixation cross, yielding a total of 190 trials (50 High-risk, 50 Low-risk, 50 Control and 40 Null trials in total). 4.2 min runs were comprised of 20 12-second trials including 6 high-risk trials, 6 low-risk trials, 4 control trials and 4 null trials, yielding a total of 190 trials (60 High-risk, 60 Low-risk, 40 Control and 40 Null trials in total). Trial occurrence was randomized and counterbalanced, such that each condition was followed by all other conditions, as well as null trials, an equal number of times.

4.4. Behavioral decision-making model

According to Expected Utility Theory (Bernoulli, 1763/1958), behavior is guided by the magnitude of anticipated gains, x, and the probability, p, of receiving a rewarding outcome, such that decision-makers tend to chose the alternative with the highest expected utility (EU), provided by:

$$EU = \sum_{i=1}^{n} u(x_i) \times p_i. \quad (1)$$

The utility of obtaining outcome x_i, $u(x_i)$, can be influenced by subjective factors determining the "moral" value of a lottery (Schunk and Betsch, 2006; Trepel et al., 2005). An influential factor is a person's level of risk-aversion. According to EUT, risk-aversion is typically estimated as the curvature of the expected utility function (Arrow, 1965; Pratt, 1964). Utility functions can be expressed as power functions, such that the utility of a certain amount, x, is provided by:

$$u(x) = x^{\alpha} \quad (2)$$

where α is the exponent reflecting the curvature of the utility function and, consequently, level of risk-aversion. Linearity of

the utility function ($\alpha=1$) represents risk-neutrality and indicates that the utility of a given lottery is determined by the multiplication of gain magnitude and probability. Of note, deviations from linearity indicate the presence of subjective factors (Schunk and Betsch 2006). A risk-averse individual has a concave utility function with an $\alpha<1$, while a risk-seeking individual has a convex utility function with an $\alpha>1$. Utility functions are typically concave in the domain of gains (e.g. Kahneman and Tverksy, 1979; Tversky and Kahneman, 1992), but heterogeneity across individuals has been reported previously (e.g. Fetherstonhaugh et al., 1997; Schunk and Betsch, 2006).

We employed nonlinear logistic regression analysis to extract the curvature of each participant's utility function for gains from participants' choices between monetary lotteries involving differing degrees of risk. Behavioral data was sorted according to level of risk selected by participants. Risk was defined as the variance of the outcome of the selected option, as done previously (Preuschoff et al., 2006; Tobler et al., 2007; Xue et al., 2009) and was calculated using the following equation:

$$\text{Risk} = \left[(1-p)^*(0-\text{EV})^2 + p^*(x-\text{EV})^2\right] \quad (3)$$

where p is the probability of the outcome, EV is the expected value and x is the magnitude of the outcome. Choices were coded as *high-risk* when subjects chose the option involving a relatively greater risk but yielding a larger payoff, while trials were coded as *low-risk* when subjects chose the lottery with relatively lower risk yielding a smaller payoff. For example, a high-risk choice involved choosing the gamble yielding $18 at a probability of 10% (risk=29.16) over the gamble yielding $2 at a probability of 90% (risk=0.36), or choosing the gamble yielding $4.5 at a probability of 40% (risk=4.86) over the gamble yielding $3 at a probability of 60% (risk=2.16). Opposite choices were coded as *low-risk* choices. Choices during control trials were not included in the regression analysis, as lotteries did not provide a difference in risk (δ_{AB}) during the control condition. Table 6 shows risk designations used in behavioral and fMRI analyses, as well as quantities reflecting experienced risk during each type of choice.

The difference in expected utility between the lotteries on a given trial i, δ_{EU} was calculated as:

$$\delta_{EU} = [p1_i \times u(x1_i)] - [p2_i \times u(x2_i)] \quad (4)$$

where $p1_i$ is the probability of winning lottery 1 (L1), $p2_i$ is the probability of winning lottery 2 (L2), $u(x1_i)$ is the utlity of anticipated gains for lottery 1, $u(x2_i)$ is the utility of anticipated gains for lottery 2. The utility of the magnitude of the anticipated gain was estimated using the power function (Eq. (2)) Finally, the probability of choosing lottery 1 was estimated using nonlinear least-squares fitting tools provided in Matlab as:

$$P_{L1} = \frac{e^{\delta}}{1+e^{\delta}} \quad (5)$$

4.5. *Behavioral performance*

Mean reaction times of each subject were calculated for each decision type and entered into a 2-way mixed Analysis of Variance (ANOVA) with CHOICE (3 levels: high-risk, low-risk and control) as the within-subjects factor and SESSION (2 levels: Brown University, Indiana University) as between-subjects factor. *Magnetic Resonance Imaging procedures*. Scanning was conducted at two research sites: Data from 4 subjects were collected with a 1.5 T Siemens Symphony MRI whole body system (Siemens Medical Systems, Erlangen, Germany) located at Memorial Hospital of Rhode Island. Gradient-echo echo-planar images (EPI) were acquired in a transverse plane by sampling thirty three axial slices (interleaved) with a thickness of 4 mm and encompassing a field of view of 192 mm with an inplane resolution of 64×64 (608–760 scans, voxel size: 3×3×4 mm, TR=3000 ms, TE=38 ms); Data from 6 additional subjects were collected using a 3 T Siemens Magnetron Trio whole body scanner (Siemens Medical Systems, Erlangen, Germany) located at Indiana University in Bloomington. Gradient-echo echo-planar images (EPI) were acquired in a transverse plane by sampling forty-two axial slices (interleaved) with a thickness of 4 mm and encompassing a field of view of 192 mm with an inplane resolution of 64×64 (860 scans, voxel size: 3×3×4 mm, TR=3000 ms, TE=30 ms).

At both locations, the task was presented with Presentation software (Neurobehavioral Systems, Albany, CA) and visual stimuli were projected onto a frosted glass screen, which the subject viewed through an angled mirror mounted to the head coil. In order to reduce eye movement artifacts, participants were instructed to focus on the fixation cross whenever presented in the experiment. Inhomogeneities in the magnetic field introduced by the participant were minimized with a standard two-dimensional head shimming protocol before each run and the anatomical data acquisition. At both sites, a three dimensional, high-resolution anatomical data set was acquired using Siemens' magnetization prepared rapid acquisition gradient echo (MPRAGE) sequence before the acquisition of functional images (TR of 1900 ms, TE of 4.15 ms, TI of 1100 ms, 1 mm isotropic voxels and a 256 mm FOV).

Table 6 – Outline of lottery pairs and risk-level associated with subject choice, experienced risk reflective of the variance of the outcome associated with the chosen option is reported in brackets.

Gamble A		Gamble B		Risk designation		
Probability	Magnitude	Probability	Magnitude	Subject chose lottery A	Subject chose lottery B	Δ_{risk} (lottery A – lottery B)
10%	$18	90%	$2	High-risk (29.16)	Low-risk (0.36)	28.8
40%	$4.5	60%	$3	High-risk (4.86)	Low-risk (2.16)	2.7
50%	$3.6	50%	$3.6	Control (3.24)	Control (3.24)	0
60%	$3	40%	$4.5	Low-risk (2.16)	High-risk (4.86)	−2.7
90%	$2	10%	$18	Low-risk (0.36)	High-risk (29.16)	−28.8

4.6. *fMRI data analysis*

4.6.1. *fMRI preprocessing*

Initial preprocessing of the data was conducted using AFNI (http://afni.nimh.nih.gov/afni). To allow for T1 equilibrium effects, the first four volumes were removed from each run. All remaining volumes underwent slice-time acquisition correction using Fourier interpolation. The functional data were then spatially aligned to the volume acquired closest to each subject's anatomical image and subsequently underwent linear detrending, outlier correction, and spatial smoothing using an isotropic Gaussian kernel (full width at half maximum (FWHM) = 6 mm). Each voxel's signal intensity was scaled to a mean of 100, after which images were normalized into stereotaxic space (Talairach and Tournoux, 1988).

4.6.2. *fMRI analysis*

To capture subjective risk preference on a given trial, trials were sorted according to type of decision made by the subject, as done for behavioral analyses and described in detail for the behavioral decision-making model. Briefly, trials were designated as *high-risk* decisions when participants chose the alternative involving the higher risk over the alternative with the lower risk, e.g. choosing 10% of $18 (risk = 29.16) over 90% of $2 (risk = 0.36), or choosing 40% of $4.5 (risk = 4.86) over 60% of $3 (risk = 2.16), while opposite choices were coded as *low-risk* decisions (see Table 6). Note that in the current study, risk categories were therefore based on participants' choices, which are reflective of risk preference on a given trial. Risk, as defined in the current study, therefore reflects whether participants chose the option with a relatively higher risk compared to the option with the relatively lower risk We therefore refer to risk as *relative behavioral risk*. The mean experienced risk was 17.01 after high-risk choices and 1.26 after low-risk choices. Control choices, while offering an intermediate risk-level, differed from risky choices mainly by providing no behavioral control over the outcome, as participants could not choose an option with relatively lower or higher risk-level (both lotteries offered the same probability and reward magnitude in this condition).

Trials in which no response was made within the 3-second period of the decision phase were removed from further analysis. The data were then analyzed using the General Linear Model and a standard two-stage mixed effects analysis. The first-level multiple regression model consisted of 8 orthogonal regressors of interest (decision phase regressors (0–3 s post trial onset, based on RT): control, low-risk, high-risk choices; anticipation phase regressors (3–9 s): control, low-risk, high-risk; outcome phase regressors (9–12 s): won, lost) and additional regressors of no interest (constant and polynomial terms) for each run to model slow signal drifts. To fully capture the decision phase and introduce jitter, hemodynamic responses during this period were modeled as convolved boxcars with a length representing the time taken to arrive at a decision on each trial (reaction times varied between 446 ms and 2594 ms in the control condition, 347 ms and 2769 ms in the LR condition and from 379 ms to 2529 ms in the HR condition). Activity during decision-making and anticipation phases was modeled in terms of risk-level selected by the subject: high-risk, low-risk and control choices. Activity during the outcome phase was modeled in terms of whether subjects won or lost.

First-level contrasts were entered into separate second-level Analyses of Covariance (ANCOVA) for each phase of the decision-making task, which included SESSION (a mean-centered dummy variable) as covariate to control for potential effects of different scanner environments. Specifically, contrasts probed for linear increases as a function of the chosen relative risk-level in the decision and anticipation periods (control (weight: −1), low-risk (weight: 0), high-risk (weight: 1)) and regions showing increased activation as a function of winning during the outcome period (winning > losing). An uncorrected p value of 0.001 was chosen as statistical significance. In addition, a cluster-size threshold of 3 was employed for all mixed effects maps. The voxelwise p value resulting from combining a threshold of $p = 0.001$ with a minimum cluster-size of 3 was estimated to be 0.0003259 by Monte Carlo simulations conducted with the AFNI program AlphaSim.

The above whole-brain analysis probed for regions encoding relative behavioral risk in decision and anticipation periods. To illustrate fMRI responses at those sites that showed significant activations during each of the task periods, a deconvolution procedure with shifted cubic spline functions was employed to model responses during high-risk, low-risk and control decisions throughout the entire task period (21 s). Specifically, the hemodynamic response for each type of choice was modeled with a basis set of seven cubic spline functions spaced one TR (3 s) apart and spanning the interval from 0 to 21 s post trial onset. In order to create reconstructed event-related responses on a 1 s temporal grid, the set of fitted spline functions was resampled at a temporal resolution of 1 s and averaged within each ROI. Of note, this model was independent of the model used to select ROIs. In this manner, we were able to illustrate estimated responses without making any assumptions about the time course of activation (i.e., the canonical hemodynamic response). Importantly, these deconvolved responses did not assume that activity followed a linear increase as a function of risk, nor that anticipation activity was maintained during the interstimulus interval separating decision and outcome periods. Similarly, to illustrate activity in regions activated during the outcome period, a separate deconvolution procedure was employed modeling responses during winning and losing throughout the entire task period.

Additionally, to illustrate the *degree* to which areas distinguish between risk-level during choice and anticipation, two independent ROI analyses were carried out: (1) Trend analyses were conducted on the mean of activations at time points 6 and 7 s post trial onset, representing the middle two points around the expected peak response during the decision phase (Fig. 1B), as well as on the mean of activations at time points 10, 11 and 12 s post trial onset, representing the middle three points around the expected peak response during the anticipation phase (Fig. 1B). All trend analyses included SESSION as between-subjects factor to investigate potential effects of different scanning environments on activation patterns. (2) We also performed independent confirmatory parametric ROI analyses. A separate first-level model was obtained, which included parametric modulators

predictive of the chosen risk-level on each trial during decision and anticipation periods. The first-level parametric regression model consisted of 6 regressors of interest (decision phase, decision × risk, anticipation, anticipation × risk, won, lost). Risk was coded as 0 during control trials, and was equal to the variance of the chosen option on experimental trials (see Eq. (3)). Mean regression coefficients from parametric modulators, reflective of the slope of the correlation between brain activity and risk, were extracted for each region of the decision and anticipation networks and entered into confirmatory ROI analyses (Tables 2 and 4). We also performed parametric voxelwise whole-brain analyses (tables SM1 and SM2), but we focus on brain activations related to relative behavioral risk in the main paper, because these parallel our behavioral decision-making model.

Finally, in order to demonstrate activation patterns during the outcome phase and to investigate the effect of differences in scanning environments on BOLD responses during the outcome period, separate mixed ANOVAs, with OUTCOME (won, lost) as within-subjects factor and SESSION (IU, BrU) as between-subjects factor were conducted on mean activations at time points 15 and 16 s post trial onset, representing the middle two points around the expected peak response during the outcome phase (Fig. 1B). To mitigate the multiple-comparisons problem arising from conducting repeated analyses on multiple brain regions, the alpha level for statistical significance of trend analyses was Bonferroni corrected and set to 0.007 for the decision period (7 comparisons) and 0.008 for anticipation and outcome periods (6 comparisons). Exact p values are provided when values did not reach this significance level. Additionally, all p values less than 0.05 are referred to as near-significant in the context of Bonferroni corrections.

Acknowledgments

We thank Gregory Berns, Monica Capra, Eswar Damaraju, Sara Moore, Giuseppe Pagnoni and Luiz Pessoa for helpful advice and Vishnu Murti for help with data collection. We are also grateful to the reviewers for their insightful comments that significantly improved the quality of this paper. The research described in this paper was supported by a grant from the American Psychological Association to J.B.E. and by a Fellowship in the Training Program in the Neurobiology of Drug Abuse to J.B.E. (T32 DA014040).

REFERENCES

Abdellaoui, M., 2000. Parameter-free elicitation of utility and probability weighting functions. Manag. Sci. 46 (11), 1497–1512.

Arkadir, D., Morris, G., Vaadia, E., Bergman, H., 2004. Independent coding of movement direction and reward prediction by single pallidal neurons. J. Neurosci. 24 (45), 10047–10056.

Aron, A., Fisher, H., Mashek, D.J., Strong, G., Li, H., Brown, L.L., 2005. Reward, motivation, and emotion systems associated with early-stage intense romantic love. J. Neurophysiol. 94 (1), 327–337.

Arrow, K.J., 1965. Aspects of the Theory of Risk Bearing. Yrjö Hahnsson Foundation, Helsinki.

Barsky, R.B., Kimball, M.S., Juster, F.T., Shapiro, M.D., 1997. Preference parameters and behavioral heterogeneity: an experimental approach in the health and retirement survey. Q. J. Econ. 112, 537–579.

Beetsma, R.M.W.J., Schotman, P.C., 2001. Measuring risk attitudes in a natural experiment: data from the television game show Lingo. Econ. J. 111 (474), 821–848.

Bernoulli, D., 1763/1958. Exposition of a new theory on the measurement of risk. Econometrica 22, 23–36.

Berns, G.S., McClure, S.M., Pagnoni, G., Montague, P.R., 2001. Predictability modulates human brain response to reward. J. Neurosci. 21 (8), 2793–2798.

Berns, G.S., Chappelow, J., Cekic, M., Zink, C.F., Pagnoni, G., Martin-Skurski, M.E., 2006. Neurobiological substrates of dread. Science 312 (5774), 754–758.

Breiter, H.C., Aharon, I., Kahneman, D., Dale, A., Shizgal, P., 2001. Functional imaging of neural responses to expectancy and experience of monetary gains and losses. Neuron 30 (2), 619–639.

Bush, G., Luu, P., Posner, M.I., 2000. Cognitive and emotional influences in anterior cingulate cortex. Trends Cogn. Sci. 4 (6), 215–222.

Bush, G., Vogt, B.A., Holmes, J., Dale, A.M., Greve, D., Jenike, M.A., Rosen, B.R., 2002. Dorsal anterior cingulate cortex: a role in reward-based decision making. Proc. Natl. Acad. Sci. U. S. A. 99 (1), 523–528.

Camerer, C.F., 2003. Psychology and economics. Strategizing in the brain. Science 300 (5626), 1673–1675.

Casey, B.J., Forman, S.D., Franzen, P., Berkowitz, A., Braver, T.S., Nystrom, L.E., Thomas, K.M., Noll, D.C., 2001. Sensitivity of prefrontal cortex to changes in target probability: a functional MRI study. Hum. Brain Mapp. 13 (1), 26–33.

Castelli, F., Happe, F., Frith, U., Frith, C., 2000. Movement and mind: a functional imaging study of perception and interpretation of complex intentional movement patterns. Neuroimage 12 (3), 314–325.

Chandrasekhar, P.V., Capra, C.M., Moore, S., Noussair, C., Berns, G.S., 2008. Neurobiological regret and rejoice functions for aversive outcomes. Neuroimage 39 (3), 1472–1484.

Cohen, M.X., Ranganath, C., 2005. Behavioral and neural predictors of upcoming decisions. Cogn. Affect Behav. Neurosci. 5, 117–126.

Corbetta, M., Kincade, J.M., Ollinger, J.M., McAvoy, M.P., Shulman, G.L., 2000. Voluntary orienting is dissociated from target detection in human posterior parietal cortex. Nat. Neurosci. 3 (3), 292–297.

Critchley, H.D., Mathias, C.J., Dolan, R.J., 2001. Neural activity in the human brain relating to uncertainty and arousal during anticipation. Neuron 29 (2), 537–545.

Delgado, M.R., Stenger, V.A., Fiez, J.A., 2004. Motivation-dependent responses in the human caudate nucleus. Cereb. Cortex 14 (9), 1022–1030.

Delgado, M.R., Frank, R.H., Phelps, E.A., 2005a. Perceptions of moral character modulate the neural systems of reward during the trust game. Nat. Neurosci. 8 (11), 1611–1618.

Delgado, M.R., Miller, M.M., Inati, S., Phelps, E.A., 2005b. An fMRI study of reward-related probability learning. Neuroimage 24 (3), 862–873.

Delgado, M.R., Gillis, M.M., Phelps, E.A., 2008. Regulating the expectation of reward via cognitive strategies. Nat. Neurosci. 11 (8), 880–881.

Elliott, R., Friston, K.J., Dolan, R.J., 2000. Dissociable neural responses in human reward systems. J. Neurosci. 20 (16), 6159–6165.

Engelmann, J.B., Damaraju, E., Padmala, S., Pessoa, L., 2009. Combined effects of attention and motivation on visual task performance: transient and sustained motivational effects. Front. Hum. Neurosci 3, 4. doi:10.3389/neuro.09.004.2009.

Ernst, M., Nelson, E.E., McClure, E.B., Monk, C.S., Munson, S., Eshel, N., Zarahn, E., Leibenluft, E., Zametkin, A., Towbin, K., et al.,

2004. Choice selection and reward anticipation: an fMRI study. Neuropsychologia 42 (12), 1585–1597.
Eshel, N., Nelson, E.E., Blair, R.J., Pine, D.S., Ernst, M., 2007. Neural substrates of choice selection in adults and adolescents: development of the ventrolateral prefrontal and anterior cingulate cortices. Neuropsychologia 45, 1270–1279.
Fetherstonhaugh, D., Slovic, P., Johnson, S., Friedrich, J., 1997. Insensitivity to the value of human life: a study of psychophysical numbing. J. Risk Uncertain. 14, 283–300.
Gonzales, R., Wu, G., 1999. On the shape of the probability weighting function. Cogn. Psychol. 38, 129–166.
Gusnard, D.A., Raichle, M.E., 2001. Searching for a baseline: functional imaging and the resting human brain. Nat. Rev. Neurosci. 2 (10), 685–694.
Gusnard, D.A., Akbudak, E., Shulman, G.L., Raichle, M.E., 2001. Medial prefrontal cortex and self-referential mental activity: relation to a default mode of brain function. Proc. Natl. Acad. Sci. U. S. A. 98 (7), 4259–4264.
Hollerman, J.R., Tremblay, L., Schultz, W., 1998. Influence of reward expectation on behavior-related neuronal activity in primate striatum. J. Neurophysiol. 80 (2), 947–963.
Hopfinger, J.B., Buonocore, M.H., Mangun, G.R., 2000. The neural mechanisms of top-down attentional control. Nat. Neurosci. 3 (3), 284–291.
Huettel, S.A., 2006. Behavioral, but not reward, risk modulates activation of prefrontal, parietal, and insular cortices. Cogn. Affect. Behav. Neurosci. 6 (2), 141–151.
Huettel, S.A., Song, A.W., McCarthy, G., 2005. Decisions under uncertainty: probabilistic context influences activation of prefrontal and parietal cortices. J. Neurosci. 25 (13), 3304–3311.
Huettel, S.A., Stowe, C.J., Gordon, E.M., Warner, B.T., Platt, M.L., 2006. Neural signatures of economic preferences for risk and ambiguity. Neuron 49 (5), 765–775.
Johnson, S.C., Baxter, L.C., Wilder, L.S., Pipe, J.G., Heiserman, J.E., Prigatano, G.P., 2002. Neural correlates of self-reflection. Brain 125 (Pt 8), 1808–1814.
Kable, J.W., Glimcher, P.W., 2007. The neural correlates of subjective value during intertemporal choice. Nat. Neurosci. 10 (12), 1625–1633.
Kachelmeier, S.J., Shehata, M., 1992. Examining risk preferences under high monetary incentives: experimental evidence from the People's Republic of China. Am. Econ. Rev. 82 (5), 1120–1141.
Kahneman, D., Tverksy, A., 1979. Prospect theory: an analysis of decision under risk. Econometrica 47, 263–291.
Kerns, J.G., Cohen, J.D., MacDonald III, A.W., Cho, R.Y., Stenger, V.A., Carter, C.S., 2004. Anterior cingulate conflict monitoring and adjustments in control. Science 303 (5660), 1023–1026.
Kircher, T.T., Senior, C., Phillips, M.L., Rabe-Hesketh, S., Benson, P.J., Bullmore, E.T., Brammer, M., Simmons, A., Bartels, M., David, A.S., 2001. Recognizing one's own face. Cognition 78 (1), B1–B15.
Kircher, T.T., Brammer, M., Bullmore, E., Simmons, A., Bartels, M., David, A.S., 2002. The neural correlates of intentional and incidental self processing. Neuropsychologia 40 (6), 683–692.
Knutson, B., Cooper, J.C., 2005. Functional magnetic resonance imaging of reward prediction. Curr. Opin. Neurol. 18 (4), 411–417.
Knutson, B., Peterson, R., 2005. Neurally reconstructing expected utility. Games Econom. Behav. 52, 305–315.
Knutson, B., Westdorp, A., Kaiser, E., Hommer, D., 2000. FMRI visualization of brain activity during a monetary incentive delay task. NeuroImage 12, 20–27.
Knutson, B., Adams, C.M., Fong, G.W., Hommer, D., 2001a. Anticipation of increasing monetary reward selectively recruits nucleus accumbens. J. Neurosci. 21, RC159.
Knutson, B., Fong, G.W., Adams, C.M., Varner, J.L., Hommer, D., 2001b. Dissociation of reward anticipation and outcome with event-related fMRI. Neuroreport 12 (17), 3683–3687.
Knutson, B., Fong, G.W., Bennett, S.M., Adams, C.M., Hommer, D., 2003. A region of mesial prefrontal cortex tracks monetarily rewarding outcomes: characterization with rapid event-related fMRI. Neuroimage 18 (2), 263–272.
Knutson, B., Taylor, J., Kaufman, M., Peterson, R., Glover, G., 2005. Distributed neural representation of expected value. J. Neurosci. 25 (19), 4806–4812.
Knutson, B., Rick, S., Wimmer, G.E., Prelec, D., Loewenstein, G., 2007. Neural predictors of purchases. Neuron 53 (1), 147–156.
Krawczyk, D.C., 2002. Contributions of the prefrontal cortex to the neural basis of human decision making. Neurosci. Biobehav. Rev. 26 (6), 631–664.
Kuhnen, C.M., Knutson, B., 2005. The neural basis of financial risk taking. Neuron 47 (5), 763–770.
Liu, X., Powell, D.K., Wang, H., Gold, B.T., Corbly, C.R., Josephs, J.E., 2007. Functional dissociation in frontal and striatal areas for processing of positive and negative reward information. J. Neurosci. 27 (17), 4587–4597.
Loewenstein, G.F., Weber, E.U., Hsee, C.K., Welch, N., 2001. Risk as feelings. Psychol. Bull. 127 (2), 267–286.
Maddock, R.J., 1999. The retrosplenial cortex and emotion: new insights from functional neuroimaging of the human brain. Trends Neurosci. 22 (7), 310–316.
Maddock, R.J., Garrett, A.S., Buonocore, M.H., 2003. Posterior cingulate cortex activation by emotional words: fMRI evidence from a valence decision task. Hum. Brain Mapp. 18 (1), 30–41.
McAlonan, G.M., Robbins, T.W., Everitt, B.J., 1993. Effects of medial dorsal thalamic and ventral pallidal lesions on the acquisition of a conditioned place preference: further evidence for the involvement of the ventral striatopallidal system in reward-related processes. Neuroscience 52 (3), 605–620.
McClure, S.M., Berns, G.S., Montague, P.R., 2003. Temporal prediction errors in a passive learning task activate human striatum. Neuron 38 (2), 339–346.
McCoy, A.N., Platt, M.L., 2005. Risk-sensitive neurons in macaque posterior cingulate cortex. Nat. Neurosci. 8 (9), 1220–1227.
McCoy, A.N., Crowley, J.C., Haghighian, G., Dean, H.L., Platt, M.L., 2003. Saccade reward signals in posterior cingulate cortex. Neuron 40 (5), 1031–1040.
Mellers, B.A., 2000. Choice and the relative pleasure of consequences. Psychol. Bull. 126 (6), 910–924.
Mellers, B.A., 2001. Anticipated emotions as guides to choice. Curr. Dir. Psychol. Sci. 10 (6), 210–214.
Menon, M., Jensen, J., Vitcu, I., Graff-Guerrero, A., Crawley, A., Smith, M.A., Kapur, S., 2007. Temporal difference modeling of the blood-oxygen level dependent response during aversive conditioning in humans: effects of dopaminergic modulation. Biol. Psychiatry 62 (7), 765–772.
Mirenowicz, J., Schultz, W., 1996. Preferential activation of midbrain dopamine neurons by appetitive rather than aversive stimuli. Nature 379, 449–451.
Montague, P.R., Berns, G.S., 2002. Neural economics and the biological substrates of valuation. Neuron 36, 265–284.
Montague, P.R., Hyman, S.E., Cohen, J.D., 2004. Computational roles for dopamine in behavioural control. Nature 431 (7010), 760–767.
Nagahama, Y., Okada, T., Katsumi, Y., Hayashi, T., Yamauchi, H., Sawamoto, N., Toma, K., Nakamura, K., Hanakawa, T., Konishi, J., et al., 1999. Transient neural activity in the medial superior frontal gyrus and precuneus time locked with attention shift between object features. Neuroimage 10 (2), 193–199.
Ochsner, K.N., Knierim, K., Ludlow, D.H., Hanelin, J., Ramachandran, T., Glover, G., Mackey, S.C., 2004a. Reflecting upon feelings: an fMRI study of neural systems supporting the attribution of emotion to self and other. J. Cogn. Neurosci. 16 (10), 1746–1772.

Ochsner, K.N., Ray, R.D., Cooper, J.C., Robertson, E.R., Chopra, S., Gabrieli, J.D., Gross, J.J., 2004b. For better or for worse: neural systems supporting the cognitive down- and up-regulation of negative emotion. Neuroimage 23 (2), 483–499.

O'Doherty, J., Critchley, H., Deichmann, R., Dolan, R.J., 2003a. Dissociating valence of outcome from behavioral control in human orbital and ventral prefrontal cortices. J. Neurosci. 23 (21), 7931–7939.

O'Doherty, J.P., Dayan, P., Friston, K., Critchley, H., Dolan, R.J., 2003b. Temporal difference models and reward-related learning in the human brain. Neuron 38 (2), 329–337.

Paulus, M.P., Frank, L.R., 2006. Anterior cingulate activity modulates nonlinear decision weight function of uncertain prospects. NeuroImage 30, 668–677.

Paulus, M.P., Hozack, N., Zauscher, B., McDowell, J.E., Frank, L., Brown, G.G., Braff, D.L., 2001. Prefrontal, parietal, and temporal cortex networks underlie decision-making in the presence of uncertainty. Neuroimage 13 (1), 91–100.

Paulus, M.P., Rogalsky, C., Simmons, A., Feinstein, J.S., Stein, M.B., 2003. Increased activation in the right insula during risk-taking decision making is related to harm avoidance and neuroticism. Neuroimage 19 (4), 1439–1448.

Paulus, M.P., Feinstein, J.S., Leland, D., Simmons, A.N., 2005. Superior temporal gyrus and insula provide response and outcome-dependent information during assessment and action selection in a decision-making situation. Neuroimage 25 (2), 607–615.

Pessoa, L., Kastner, S., Ungerleider, L.G., 2002. Attentional control of the processing of neural and emotional stimuli. Brain Res. Cogn. Brain Res. 15 (1), 31–45.

Phan, K.L., Taylor, S.F., Welsh, R.C., Ho, S.H., Britton, J.C., Liberzon, I., 2004. Neural correlates of individual ratings of emotional salience: a trial-related fMRI study. NeuroImage 21, 768–780.

Platt, M.L., 2002. Neural correlates of decisions. Curr. Opin. Neurobiol. 12 (2), 141–148.

Platt, M.L., Glimcher, P.W., 1999. Neural correlates of decision variables in parietal cortex. Nature 400, 233–238.

Platt, M.L., Huettel, S.A., 2008. Risky business: the neuroeconomics of decision making under uncertainty. Nat. Neurosci. 11 (4), 398–403.

Pratt, J.W., 1964. Risk aversion in the small and in the large. Econometrica 32, 122–136.

Preuschoff, K., Bossaerts, P., Quartz, S.R., 2006. Neural differentiation of expected reward and risk in human subcortical structures. Neuron 51, 381–390.

Ridderinkhof, K.R., Ullsperger, M., Crone, E.A., Nieuwenhuis, S., 2004. The role of the medial frontal cortex in cognitive control. Science 306 (5695), 443–447.

Rogers, R.D., Owen, A.M., Middleton, H.C., Williams, E.J., Pickard, J.D., Sahakian, B.J., Robbins, T.W., 1999. Choosing between small, likely rewards and large, unlikely rewards activates inferior and orbital prefrontal cortex. J. Neurosci. 20 (19), 9029–9038.

Rogers, R.D., Ramnani, N., Mackay, C., Wilson, J.L., Jezzard, P., Carter, C.S., Smith, S.M., 2004. Distinct portions of anterior cingulate cortex and medial prefrontal cortex are activated by reward processing in separable phases of decision-making cognition. Biol. Psychiatry 55 (6), 594–602.

Schultz, W., Dickinson, A., 2000. Neuronal coding of prediction errors. Annu. Rev. Neurosci. 23, 473–500.

Schultz, W., Apicella, P., Scarnati, E., Ljungberg, T., 1992. Neuronal activity in monkey ventral striatum related to the expectation of reward. J. Neurosci. 12 (12), 4595–4610.

Schultz, W., Dayan, P., Montague, P.R., 1997. A neural substrate of prediction and reward. Science 275, 1593–1599.

Schunk, D., Betsch, C., 2006. Explaining heterogeneity in utility functions by individual differences in decision modes. J. Econ. Psychol. 27, 386–401.

Seymour, B., O'Doherty, J.P., Dayan, P., Koltzenburg, M., Jones, A.K., Dolan, R.J., Friston, K.J., Frackowiak, R.S., 2004. Temporal difference models describe higher-order learning in humans. Nature 429 (6992), 664–667.

Shulman, G.L., Corbetta, M., Buckner, R.L., Raichle, M.E., Fiez, J.A., Miezin, F.M., Petersen, S.E., 1997. Top-down modulation of early sensory cortex. Cereb. Cortex 7 (3), 193–206.

Simmons, A., Matthews, S.C., Paulus, M.P., Stein, M.B., 2008. Intolerance of uncertainty correlates with insula activation during affective ambiguity. Neurosci. Lett. 430 (2), 92–97.

Small, D.M., Zatorre, R.J., Dagher, A., Evans, A.C., Jones-Gotman, M., 2001. Changes in brain activity related to eating chocolate: from pleasure to aversion. Brain 124 (Pt 9), 1720–1733.

Small, D.M., Gitelman, D., Simmons, K., Bloise, S.M., Parrish, T., Mesulam, M.M., 2005. Monetary incentives enhance processing in brain regions mediating top-down control of attention. Cereb. Cortex 15 (12), 1855–1865.

Sugiura, M., Watanabe, J., Maeda, Y., Matsue, Y., Fukuda, H., Kawashima, R., 2005. Cortical mechanisms of visual self-recognition. Neuroimage 24 (1), 143–149.

Sugiura, M., Sassa, Y., Jeong, H., Miura, N., Akitsuki, Y., Horie, K., Sato, S., Kawashima, R., 2006. Multiple brain networks for visual self-recognition with different sensitivity for motion and body part. Neuroimage 32 (4), 1905–1917.

Talairach, J., Tournoux, P., 1988. Co-planar Stereotaxic Atlas of the Human Brain. Thieme, Stuttgart.

Tanaka, S.C., Balleine, B.W., O'Doherty, J.P., 2008. Calculating consequences: brain systems that encode the causal effects of actions. J. Neurosci. 28 (26), 6750–6755.

Tobler, P.N., Fletcher, P.C., Bullmore, E.T., Schultz, W., 2007. Learning-related human brain activations reflecting individual finances. Neuron 54, 167–175.

Tom, S.M., Fox, C.R., Trepel, C., Poldrack, R.A., 2007. The neural basis of loss aversion in decision-making under risk. Science 315 (5811), 515–518.

Trepel, C., Fox, C.R., Poldrack, R.A., 2005. Prospect theory on the brain? Toward a cognitive neuroscience of decision under risk. Brain Res. Cogn. Brain Res. 23 (1), 34–50.

Tricomi, E.M., Delgado, M.R., Fiez, J.A., 2004. Modulation of caudate activity by action contingency. Neuron 41 (2), 281–292.

Tversky, A., Fox, C.R., 1994. Weighting risk and uncertainty. Psychol. Rev. 102, 269–283.

Tversky, A., Kahneman, D., 1992. Advances in prospect theory. Cumulative representation of uncertainty. J. Risk Uncertain. 5, 297–323.

Tversky, A., Kahnemann, D., 1981. The framing of decisions and the psychology of choice. Science 211, 453–458.

Vogt, B.A., Berger, G.R., Derbyshire, S.W., 2003. Structural and functional dichotomy of human midcingulate cortex. Eur. J. Neurosci. 18 (11), 3134–3144.

Vogt, B.A., Vogt, L., Laureys, S., 2006. Cytology and functionally correlated circuits of human posterior cingulate areas. Neuroimage 29 (2), 452–466.

von Neumann, J., Morgenstern, O., 1944. Theory of Games and Economic Behavior. Princeton University Press, Princeton.

Vorhold, V., Giessing, C., Wiedemann, P.M., Schutz, H., Gauggel, S., Fink, G.R., 2007. The neural basis of risk ratings: evidence from a functional magnetic resonance imaging (fMRI) study. Neuropsychologia 45 (14), 3242–3250.

Xue, G., Lu, Z., Levin, I.P., Weller, J.A., Li, X., Bechara, A., 2009. Functional dissociations of risk and reward processing in the medial prefrontal cortex. Cereb. Cortex 19, 1019–1027.

Yarkoni, T., in press. Big correlations in little studies: Inflated fMRI correlations reflect low statistical power. Commentary on Vul et al (2009). Perspectives on Psychological Science. doi:10.1111/j.1745-6924.2009.01127.x.

Zink, C.F., Pagnoni, G., Martin, M.E., Dhamala, M., Berns, G.S., 2003. Human striatal response to salient nonrewarding stimuli. J. Neurosci. 23 (22), 8092–8097.

Zink, C.F., Pagnoni, G., Martin-Skurski, M.E., Chappelow, J.C., Berns, G.S., 2004. Human striatal responses to monetary reward depend on saliency. Neuron 42 (3), 509–517.

Zysset, S., Huber, O., Ferstl, E., von Cramon, D.Y., 2002. The anterior frontomedian cortex and evaluative judgment: an fMRI study. Neuroimage 15 (4), 983–991.